ENZYME-BASED PRODUCTION OF NANOCELLULOSE FROM SOYBEAN HULLS AS A GREEN FILLER FOR RUBBER COMPOUNDING

A Thesis

Presented to

The Graduate Faculty of The University of Akron

In Partial Fulfillment

of the Requirements for the Degree

Master of Science

Vamsi Bhadriraju

December, 2020

ENZYME-BASED PRODUCTION OF NANOCELLULOSE FROM SOYBEAN HULLS AS A GREEN FILLER FOR RUBBER COMPOUNDING

Vamsi Bhadriraju

Thesis

Approved:

_____	_____
Advisor Dr. Lu-Kwang Ju	Department Chair Dr. Lu-Kwang Ju
_____	_____
Committee Member Dr. Jie Zheng	Dean of the College Dr. Craig C. Menzemer
_____	_____
Committee Member Dr. Qixin Zhou	Dean of the Graduate School Dr. Marnie M. Saunders
	_____
	Date

ABSTRACT

Nanocellulose has been investigated for use in food packaging, biomedical applications, and electronics. This work attempted to isolate and evaluate crystalline nanocellulose from soybean hulls in the form of cellulose nanofibrils (CNFs) as reinforcing fillers in natural rubber composites. CNFs and nanocrystalline cellulose (CNCs) have previously been derived from different types of lignocellulosic biomass. Previous work in this area used alkali pretreatments and acid hydrolysis to break down the complex network of cellulose, hemicellulose, and lignin present in plant cell walls. CNCs and CNFs have previously been isolated using high shear microfluidization, cryocrushing, freeze drying, and ultrafiltration. In this work, enzyme cocktails of carbohydrases produced from *Aspergillus niger* were used to hydrolyze the polysaccharides in soybean hull and soybean flour. Solids were separated from soluble sugars and other components after enzyme hydrolysis for 24 hours, and these washed solids were treated with sonication, blending, and homogenization to reduce the size of these solids. Particle size analysis showed that enzyme hydrolysis did indeed generate nanoparticles, the majority of which were between 150-200 nm. The quantity of these insoluble nanoparticles was found to be small, however, relative to that of solids and seed coat fragments approximately 100-200 μm in length. Further analysis with microscopy and SEM imaging revealed that the enzyme

hydrolysis was able to cleave sclereid structures from the seed coat and breakdown soybean hull into fragments. Smaller particle size loading at the beginning of enzyme hydrolysis was found to release more sugar, so intermediate sizes were sieved in order to maximize solids recovery and minimize sugar release. These washed and mechanically treated solids were next mixed at alkaline pH (9.8–10) with natural rubber latex and oven dried overnight to create rubber composites. The resulting composites were masticated, vulcanized, and tensile tested in order to evaluate the efficacy of treated soybean hull solids as a reinforcing filler in natural rubber at 30 parts per hundred rubber (phr). Tensile testing results revealed that there was only an improvement of 3 MPa when compared to natural rubber, while rubber reinforced with carbon black improved tensile strength by a factor of 1.5. The results of this project showed that fillers derived through enzymatic hydrolysis and mechanical treatment of soybean hull marginally improve the tensile strength of natural rubber. It is suggested for future work that iterations of size reduction and filtration are performed to ensure that CNFs are the only solids in filler suspensions when compounded with natural rubber.

DEDICATION

I dedicate this thesis to my late maternal and paternal grandparents, and my mother and father for their lifelong support of my academic career.

ACKNOWLEDGEMENTS

I would like to thank my graduate advisor, Dr. Lu-Kwang Ju, for his guidance throughout this project and for financially supporting me during my time at the University of Akron. I would like to acknowledge the help and mentorship of older labmates, Ashwin Sancheti and Krutika Invally Baliga, who assisted me immensely when I first started the graduate program. I would like to thank the Department of Chemical, Biomolecular and Corrosion Engineering for providing a top tier learning environment and giving me the tools to become a better researcher. I would also like to thank Dr. Jie Zheng and Dr. Qixin Zhou for agreeing to serve on my committee.

TABLE OF CONTENTS

LIST OF FIGURES

LIST OF TABLES

Table Page

CHAPTER I

ENZYME HYDROLYSIS AND SIZE REDUCTION OF SOYBEAN HULL

Nanoparticle production been the focal point of research for recent decades. Nanoparticles are defined as particles that have one dimension, length or width, in the nanometer range (Missoum, 2013). Nanocellulose has shown great versatility in polymer products and has been used together with thermoplastics. A few examples of nanocellulose use has been demonstrated in nylons, polysulfone, and polypropylene for use in polymer composites (Kargarzadeh et al., 2018). Furthermore, nanocellulose has shown promise in biomedical applications as nanocellulose hydrogels. These hydrogels were used in 3D cell culture, would dressings (cell regeneration), and tissue engineering scaffolds (Curvello et al., 2019).

In recent years, lignocellulosic biomass has been studied for creating nano- and micro-crystalline particles branching off from the research into this topic to produce value added products and biofuels (Kargarzadeh, 2018). In lignocellulosic biomass, cell walls are comprised of polysaccharides: cellulose, hemicellulose, and lignin. Cellulose exists in tandem with hemicellulose and the phenolic complex network of lignin.

1.1 Introduction

1.1.1 Production of Nanocellulose

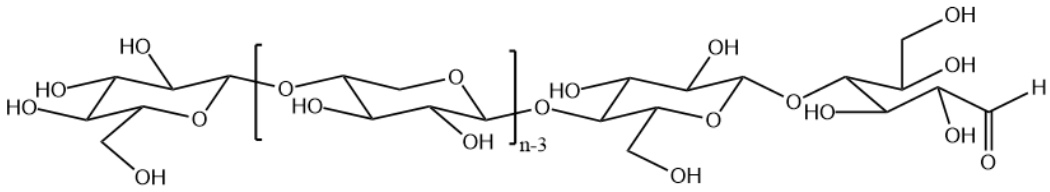

Figure 1-1. The cellulose polymer, drawn with chair conformations connected by β-1,4-glycosidic linkages. This diagram of cellulose was recreated in ChemDraw from Phanthong et al. (2018).

The repeating unit in the cellulose molecule shown above is the anhydroglucose unit (AGU) (Fig. 1-1). The group left of the AGU unit is the non-reducing end and the final group on the right side is known as the reducing end of the biopolymer (Kalia et al., 2011).

Hemicellulose is polymer consisting of various five- and six-carbon sugars. The hydrolysis of cellulose thus generates monomeric glucose and that of hemicellulose generations the five-carbon sugars xylose, arabinose, and the six-carbon sugars mannose, hexose, glucose, and galactose (Isikgor & Becer, 2015). Many research groups have investigated pretreatment methods to breakdown lignocellulosic biomass.

Research into alkali pretreatment and hydrolysis of lignocellulosic biomass into fermentable sugars was toward the application of liquid biofuels (Agbor et al., 2011). The issue with alkali pretreatment and steam explosion techniques was that the lignin degradation released many inhibitors, such as furfurals and phenolic compounds, which are known to be detrimental to fermentation (Islam et al., 2018).

A major development in the utilization of biomass wastes has been the isolation of cellulose nanocrystals. Isolation of cellulose has shown the presence of crystalline and amorphous divisions in the cellulose chain. It was learned that amorphous regions were more accessible to acid molecules aiding in the hydrolysis of cellulose chain to the glucose monomers that build the molecules (Garcia et al., 2015). Early work succeeded in isolating cellulose to a micrometer level (Merci et al., 2015). Recent work in the past decade has revealed that acidic and enzymatic processes show great potential in reducing the size of cellulose chains (Martelli-Tosi et al., 2016). These cellulose nanocrystals derived through acidic means show rod-sphere network morphologies when characterized through scanning electron microscopy (Lu & Hsieh, 2010). The major issue with these processes is the use of high acid concentrations (64-65 w/v% sulfuric acid), freeze drying with liquid nitrogen, and extensive centrifugation and ultrafiltration techniques that result in low yield (Flauzino Neto et al., 2013). In addition to this low throughput, the drying of nanocrystalline cellulose results in aggregation due to the hydrophilic nature of cellulose. Drying

of CNFs has been also been conducted with oven drying, freeze drying, supercritical drying, and spray-drying (Peng, 2012).

The issues in previous work seen with drying of nanocellulose poses a problem for the use of nanoparticles in hydrophobic polymer composites. Many polymers are hydrocarbon-rich in their backbones, unless they are functionalized or oxidized in chemical treatments (Dong et al., 2012). This drying issue has been circumvented by functionalizing either the nanoparticles or the basis of the polymer composite.

Major sources for nano and micro-crystalline cellulose right now range from plants, algae, and bacteria. Micro and nano-crystalline cellulose are popularly derived from plants like cotton linters that have high degree of polymerization (dp) of cellulose, such as 10000-15000 dp (Kalia et al, 2011).

The structure of cellulose within plants has been found to exist as elementary fibrils 2-20 nm in length aggregated in microfibrils through van der waals forces. These microfibrils are packed into highly-ordered crystalline areas and less-ordered amorphous regions. These microfibrils bundle into larger microfibril units, which then comprise what are known as cellulose fibers. Cellulose nano crystals (CNCs) were first isolated in 1951 and as mentioned before are often isolated as stiff, rod-like particles with widths of 3-50 nm and lengths of 5-300 nm depending on the application, process, or desired aspect ratio and raw material (Ranby, 1951). Because of the high surface area, CNCs have a high modulus (up to 1 GPa) and applications for reinforcing composites (Mishra et al., 2018). As mentioned previously, the hydrophilic nature of this

crystalline cellulose makes functionalizing these oxygen molecules necessary to improve binding with hydrophobic substrates (Ferreira et al., 2018). Some methods currently employed to functionalize nano- and micro-crystalline cellulose are chemical modification with (2,2,6,6-Tetramethylpiperidin-1-yl)oxyl, abbreviated as TEMPO oxidation, to oxidize alcohols to aldehydes and even using polyethylene glycol (PEG) grafting to stabilize CNC suspensions (George and Sabapathi, 2015).

A few recent papers have used enzymes to produce nanocellulose and mention the cross-linking between lignin and cellulose posing a problem for enzyme penetration (Karim et al., 2017). The presence of lignin poses problems for enzyme attack, and as mentioned before, also releases inhibitors. For this reason, soybean hull was determined to be the ideal starting material for nanocellulose production through enzyme hydrolysis. Soybean is rich in carbohydrate content, and soybean hull has very small lignin content.

1.1.2 Soybean Hull Background

This United States is the world leader in production of the legume soybean, *Glycine max* (Fabales: Fabaceae). In recent decades, soybeans have been investigated as rich sources of protein, as well as trace metals. The process for extracting value-added products out of soybean is currently framed around isolating streams of soybean oil (margarine) and soy protein isolate (imitation foods). The husks of the soybean are usually used as animal feed. In recent years, under-utilized waste streams from these processes have also been

investigated for purposes outside of immediate food and agriculture feed products. It is now understood that these soybean waste streams of soybean hull are good candidates for enzyme hydrolysis and fermentation purposes as second generation biofuels and other applications (Loman et al., 2016). The typical composition of soybean hull is 29-51% cellulose, 10-25% hemicellulose, 4-8% pectin, 11-15% proteins, and 1-4% lignin (Islam et al., 2017). The low lignin and high carbohydrate content of soybean hulls are the characteristics that make it a decent biomass source for use as a fermentation feedstock (Loman and Ju, 2016).

1.1.2.1 Soybean Hull Physiology

Plant cell walls are comprised of associated cellulose, hemicellulose, and lignin, hence the name lignocellulosic biomass. Lignin is a three-dimensional amorphous biopolymer comprised of 3 main monolignols, p-coumaryl alcohol, coniferyl alcohol, and sinapyl alcohol in different amounts (Phanthong et al., 2018).

Cellulosic fibers exist in a hierarchy that starts inside in the lumen, followed by the S1, S2, and S3 layers which comprise the secondary wall (Fig. 1-2). This is contained inside the primary cell wall. Along each stage of this there are helically arranged crystalline microfibers (Brinchi et al., 2013).

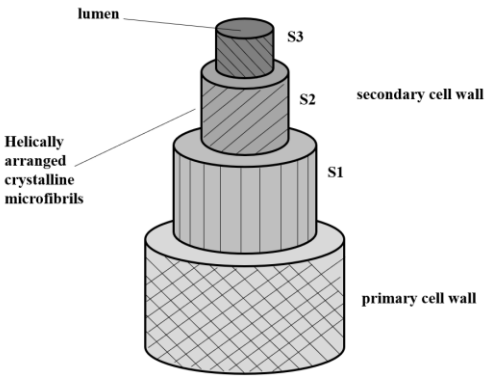

Figure 1-2. Recreated graphic showing the primary and secondary structures of cellulose in plant cell walls (Brinchi et al, 2013).

1.1.2.2 Soybean Processing

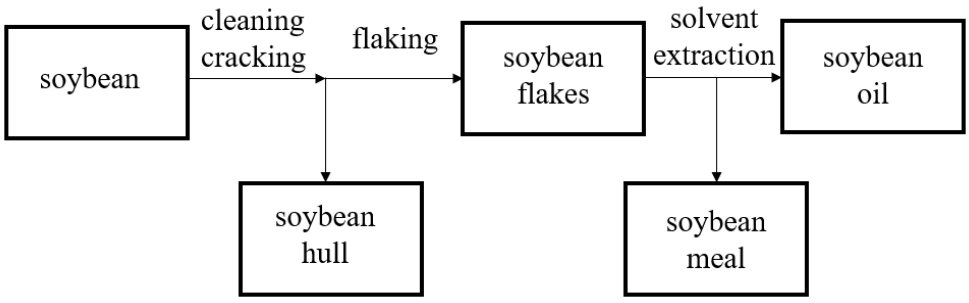

Figure 1-3. Generic process flow diagram showing how various soybean end-products are derived.

The soybean structure is based on a hierarchy or structures that protect the soybean. During soybean processing, the soybean hulls are first removed during dehulling and comprise around 8-10% of the soybean (Loman and Ju, 2016). The dehulled soybeans are next flaked and undergo a solvent extraction to produce the major commercial products of soy protein isolate (SPI), soy protein concentrate (SPC), soybean meal, and soybean oil. SPI is precipitated through pH adjustment and refined to improve the texture of meat products or

increase protein content of these products. SPC is generated through removing soluble carbohydrates through acid leeching, ethanol extraction, and heat-water leaching and is destined for use in meat products for fat and moisture retention (Loman et al., 2017). Soybean oil is used for cooking applications, and soybean meal is used in animal feeds for its large protein content, which stands around 44-49% protein.

The soybean hull is a husk that is removed during soybean processing towards other higher value products, such as soybean oil and soybean meal and full fat soy. The outer surface of the soybean structure contains lignin and palisade structures, which have an appearance of bar-like and hourglass structures, called sclereids (Ma et al., 2004). Previous work has been done into obtain cellulose nanocrystals from soybean hull for the purpose of reinforcing rubber composites. This work isolated for the same reason our lab investigated soybean hulls, high amount of cellulose (85 $\pm$ 4% cellulose, 11 $\pm$ 4% hemicellulose, 3.7 $\pm$ 0.3% lignin) (Flauzino Neto et al., 2013). One particular research group isolated CNCs from soybean hull using an intense acid hydrolysis process which involved vigorously stirring ground and sieved soybean hull with 60 wt% of H_2SO_4 per gram cellulose fiber for 30 minutes. After the hydrolysis, the reaction was stopped by dilution with deionized water ten-fold and centrifuged at 10000 rpm at 10 ºC for 15 min. Precipitate was next dialyzed with deionized water until neutral pH (due to the acidic environment of hydrolysis) then ultrasonicated in an ice bath for 15 minutes. This work does not explicitly mention the yield of CNCs, but the low loading of CNCs in the rubber composites (0 to 5

wt%) may suggest that the final yield was not sufficiently high for testing larger loadings of CNCs in the natural rubber (Flauzino Neto et al., 2016).

1.1.3 Controlled Enzyme Production in *Aspergillus niger*

Aspergillus niger is a filamentous ascomycete fungus. *A. niger* is typically used for the industrial production of citric acid. In our lab, *A. niger* strain 322 was used to produce an enzymatic cocktail produced by moderating the nitrogen and carbon biomass feed source, as well as controlling the pH of the fermentation media. This batch fermentation was conducted in two 1.5 L vessels for durations up to 3 days (or more in later studies). Activity (U/mL or FPU/mL) was assessed every during these fermentations and this data was used for later enzymatic hydrolysis experiments. The enzymes were analyzed using colorimetric assays to find the activities of α-galactosidase, sucrase, pectinase, xylanase, cellulase (Li et al., 2017). Pectinase attacks the heteropolysaccharide pectin, xylanase attacks xylan into xylose, sucrase catalyzes the hydrolysis of sucrose, and α-galactosidase hydrolyzes terminal alpha-galatosyl groups on glycolipids/glycoproteins. Pectinase, or pectic enzymes, are pectolyase, pectozyme, polygalacturonase. They are used to commercially to make jellies, jams by extracting fruit juice from fruit. Pectin is comprised galacturonic acid, which is derived from galactose. This heteropolysaccharide exists in cell walls of plants. Pectinase breaks down hemicellulose components of xylan and mannans. Cellulase is a term used for a group of multiple enzymes working synergistically,

such asendocellulases, exocellulases, celliobiases (β-glucosidase), oxidative cellulases, and cellulose phosphorlyases (Coffman, 2013).

Performing enzyme hydrolysis with these enzyme cocktails produced with *A. niger* has been shown to result in a synergistic effect, contributing to a greater breakdown of the cellulose and hemicellulose polymers (Coffman, 2013). The advantage of these enzymes working together allows a greater breakdown of biomass material during enzyme hydrolysis. The enzymes produced by *A. niger* can be used to create high-value enzyme broths, and these enzyme broths can be used downstream in large-scale hydrolyses to create fermentable sugars (Loman & Ju, 2017). *A niger* production initially causes a dip in pH as low as 2 due to the oxalic acid and gluconic acid production (Li et al., 2017). Enzyme activities were tracked to study growth, as the soybean hull and media cannot be studied for solid content as both the biomass source and fungus are solids. The results found that carbohydrase productivity for pectinase and α-galactosidase peaked in the pH range of 5-6 (Li et al., 2020).

1.1.4 Enzyme Hydrolysis of Soybean Hull

1.1.4.1 Previous Research into Applied Enzyme Hydrolysis

A considerable amount of work has been done in steam explosion and exploring alkaline pretreatments to destroy the cell wall partially before enzyme hydrolysis. It has been shown in previous research that such pretreatments maximize sugar yields from the hydrolyzed biomass (Wang et al., 2016).

In many of the previous work studying enzyme hydrolysis, pure cellulase (such as Genecor's Spezyme CP) isolated from organisms was used instead of the enzyme cocktail in our process. In many of these studies, the starting material being hydrolyzed was also microcrystalline cellulose, or highly alkali-pretreated biomass (Karim et al., 2017). A common motive in many of these hydrolysis studies was to maximize sugar release from lignocellulosic biomass to produce soluble sugars as a fermentation feedstock. The yields in the few papers that did produce nanocellulose through acid hydrolysis were found to be small and the starting material in some studies even used cellulase to breakdown already isolated starting material, such as micro-crystalline cellulose (Avicel). In our process, the goal was to minimize sugar release of glucose and retain the crystalline regions of cellulose in the form of cellulose nanofibers (CNFs). Previous work in the Ju Lab focused on using fed-batch enzyme hydrolysis to produce enriched soy protein products, as well as sugar-rich biomass hydrolysate for fermentation. Previous research from the Ju Lab at the University of Akron found that fed-batch enzyme hydrolysis improved the conversion of carbohydrates into fermentable monosugars (Loman et. al, 2017).

1.1.5 Experiment Design

The objective of the following experiments in this chapter were the converse of previously achieved objectives in the Ju Lab. Enzyme hydrolysis was used to maximize sugar release from major polysaccharides while minimizing the hydrolysis of cellulose. For this project, enzyme cocktails were deliberately

produced with low cellulase activity and moderate to high activities of xylanase, pectinase, and α-galactosidase. The main hypothesis was that the enzymes in the broth, excluding cellulase, would hydrolyze hemicellulose and amorphous regions of cellulose in the soybean hull and soybean flour when subjected to a small batch enzyme hydrolysis. By controlling the enzyme loading, it was postulated that sugar release from cellulose would be minimized and crystalline regions of cellulose would remain insoluble in the hydrolysate media. After this hydrolysis, these un-hydrolyzed solids would then be separated from soluble components and used for further particle size reduction. This project goes full circle from growing *A. niger* upon soybean hull substrate, then using the enzymes produced during fermentation in the enzyme hydrolysis.

1.2 Methods

1.2.1 Materials

Soybean hull and soybean flour were obtained from Archer Daniel Midlands company (Decatur, IL). Chemicals were purchased from Sigma Aldrich (St. Louis, MO). *Aspergillus niger* NRRL 322 was used for fermentation. Two 3.0 L bioreactors with 1.0-1.5 L working volume with controls for dissolved oxygen, agitation, pH and temperatures were used for fermentation (BioFlo 110, NewBruswick Scientific, Edison, NJ). The medium for fermentation contained $(NH_4)_2SO_4$ 1.4 g/L, KH_2PO_4 2.0 g/L, $MgSO_4 \cdot 7H_2O$ 0.3 g/L, $CaCl_2 \cdot 2H_2O$ 0.4 g/L, NH_2CONH_2 (urea) 0.3 g/L, proteose peptone 1.0 g/L, Tween 80 (0.108 g/mL) 0.2

g/L, Trace Elements 1 g/L, Soybean Hull 10 g/L. The inoculum, or preculture, was conducted at 10% of the running volume. The pH of the preculture is adjusted to 5. Shakeflask inoculum and enzyme hydrolysis were conducted in incubation shaker Thermo Scientific MaxQ 5000 Incubating/Refrigerating floor shaker (Ashville, NC). A water bath (Boekel Scientific ORS-200) was used for both thawing and incubating enzyme broth samples. Enzyme assays and other colorometric assays were conducted with a UV–vis spectrophotometer (Shimadzu UV-1601, Colombia, MD).

Soybean hydrolysate was separated with a large centrifuge 10,000 rpm (9300×g, Eppendorf 5415D). Smaller sample volumes were separated in a micro centrifuge (Eppendorf Centrifuge 5415D) (Li et al., 2020).

Soybean hydrolysate was mechanically treated with sonication, a Waring Blender, and an IKA Ultra-Turrax T18 Disperser (IKA, Wilmington, NC). Samples were analyzed with High Performance Liquid Chromatography.

A compound microscope (University of Akron, OH) was used to observe hydrolysate samples. More detailed photos were obtained using a Hitachi Tabletop SEM TM3030 magnification 15-30000x digital zoom 2x 4x; 5 kV, 15 kV voltage (Hitachi High-Technologies Corporation, Tokyo, Japan). A Wyatt Mobius Particle Size Analyzer (Wyatt Technology Corporation, Santa Barbara, CA) was used to study particle size of the hydrolysates with dynamic laser scattering.

1.2.2 Fermentation with *Aspergillus niger*

1.2.2.1 Fermentation Setup

The two bioreactors were autoclaved at 121 ºC for 90 minute autoclave liquid cycle with the soy hull and media 2 days prior to starting the inoculum. The inoculum, or preculture, was conducted at 10% of the running volume. The pH of the preculture was adjusted to 5. The larger scaled fermentation was designed by changing concentrations of nitrogen and carbon-containing compounds. The fermenter was run at 1.5 L working volume, meaning 150 mL of preculture was needed. 1.7 gram of ground soybean hull biomass, in 170 mL for preculture. After autoclaving, 3 loops of *A. niger 322* are loaded into each cooled preculture flask. The preculture was put in the shaker at 250 RPM at 25 ºC for 48 hours. The cheesecloth was fastened onto the flask with a rubber band. The extra volume (170 mL vs. 150 mL) was used to simplify withdrawal with pipette. The bioreactor was loaded with 10% (g/mL) or 150g in 1500 mL (Li et al. 2018). The correct shaft with impellers must be assembled in the fermentor, and mixing must be checked with water to find empty cavities. The dissolved oxygen probe was calibrated along with the pH probes, which were calibrated between pH 4 and 7. The acid and base lines leading to the fermenter are clamped. The media was mixed with agitation before autoclaving in order to wet all the solids. The media and clamped fermenter were subject to a 90 minute autoclave liquid cycle, a total of 2 hours total autoclave time. The ports were immediately closed after finishing autoclaving to prevent contamination. The air flow was first introduced (after

running through in high pH NaOH solution to prevent spores from air from entering the reactor) at 0.5 L/min. The agitation was next connected on the headplate until the reactor cools to room temperature. The pH probes and dissolved oxygen probes were next connected and observed for stable signals (up to 12 hours). The agitation setpoint was set to 300 and the biocommand software was initiated to track pH and dissolved oxygen (DO). The dissolved oxygen was an indicator of contamination – if values of DO dropped, it indicated that contaminating microbes were consuming oxygen in the fermentor prior to the addition of inoculum. pH was adjusted to a setpoint of 7 using concentrated sulfuric acid and NaOH base solutions (Li et al., 2020).

1.2.2.2 Sampling, Analysis, and Broth Collection

Syringe tips were sterilized with ethanol and connect to fermenter, using the 3-way valve on the sampling port and volumes of 10 mL were sampled at a time. Samples were microcentrifuged at 10000 rpm and stored for enzyme analysis and HPLC studies. After the fermentation was ceased (after from 5 – 8 days in duration, depending on the dissolved oxygen or carbohydrase production profiles), the entire volume was centrifuged using a mesh to screen the biomass from the desired enzyme broth, which was subsequently stored in the -80 ºC freezer.

1.2.3 Enzyme Hydrolysis

1.2.3.1 Enzyme Hydrolysis Design

After assaying the activities for pectinase, α-galactosidase, sucrase, xylanase, and cellulase, the collected enzyme broth was centrifuged further to separate remaining biomass. The enzyme activities of the final sample from the end of the fermentation were used as design parameters in hydrolysis. In this work, enzyme hydrolysis was designed on the basis of cellulase activity in FPU per gram cellulose. The cellulase activity (FPU/mL) was already found to be low, as seen in prior fermentation activity profiles (Li et al., 2020). By fixing the loading of the soybean hull at 100 g/L, enzyme broth volume needed was calculated using the previous finding that soybean hull contained 35.7% cellulose (Islam et al., 2017).

The equation to determine the necessary volume of enzyme was as follows,

$$enzyme\ broth\ volume = \frac{cellulase\ \left[\frac{FPU}{g\ cellulose}\right] * (cellulose\ content\ [wt\%] * biomass\ [g])}{cellulase\ activity\ \left[\frac{FPU}{mL}\right]}$$

By fixing both the cellulase design parameter (FPU per gram cellulose) and the biomass content, the volume of the enzyme broth could be back-calculated by using the measured cellulase activity (FPU/mL). After finding the appropriate enzyme volume, the hydrolysis medium was diluted with deionized water to the desired volume to achieve 100 g/L and the pH was adjusted to 4.8 (Loman et al., 2017).

1.2.3.2 Hydrolysis Protocol

Two 1 liter flasks were loaded with 100 g/L ground or sieved soybean hull or soybean flour with an enzyme volume calculated by the equation above. The enzyme was thawed and centrifuged at 10000 rpm for 10 min to obtain the supernatant. The soybean solids were first wetted with this enzyme, then diluted to 100 g/L with de-ionized water and sodium azide was added in 0.05 wt% to prevent microbial contamination. The two flasks were loaded into a shaker overnight at 50 °C and 250 rpm for 24 h. Samples were collected from the hydrolysis broth every 3-6 hours and centrifuged to track sugar concentration in the supernatant with an HPLC.

1.2.4 Separation and Treatment Studies of Soybean Hull Hydrolysate

The soy hull hydrolysates were centrifuged in 50 mL centrifuge tubes for 30 minutes at 35 mL volume. Due to poor packing, the supernatant was withdrawn using a 10 mL pipette. The resulting wet solids were mixed together in a homogenous mixture and then resuspended in dH_2O to the original weight of the hydrolysate before centrifugation. The primary reason for washing sugars from hydrolysate was to separate the high concentration of monomeric sugars and other soluble components from negative effects in later rubber compounding. In selected studies, this resuspended mixture was poured through a 254 μm (0.01”) stainless steel mesh. The dry weight of both the solid cake and the filtrate through each mesh was measured to complete mass balances and the filtrate was centrifuged

(10000 rpm, 10 min) in order to find the mass of solubles, and insolubles. This filtrate was next poured through lower range mesh sizes (139 µm, 39 µm) depending on the quantity of filtrate available.

1.2.4.1 Blending, Sonication, and Homogenization of Soybean Hydrolysate

The soy hull hydrolysate was first thawed out of the freezer at room temperature. Prior to blending, distilled water was added in controlled amounts to facilitate mixing and flow of the hydrolysate/slurry. Mechanical treatment was then applied through either a Waring blender or vortexing. Resuspended solids were blended in the Waring Blender for 15 minute intervals (10 minute cooldown period in between) for a total blending time of 30 minutes. The temperature of the blended hydrolysate was measured (it rose to approximately 75 °C). The pH of the blended hydrolysate was readjusted to 9.85 after blending for mixing with natural rubber latex to dry the rubber sample.

For sonication, washed solids were resuspended in distilled water and moved to a 400 mL beaker. The sonicator probe was immersed at a depth of 1 cm and moved around manually (the slurry was too viscous for a stir bar) to disperse solids. Sonication was performed at 180 kW in intervals of 15 minutes; after each time interval, the solids were mixed thoroughly with a spatula to assist in creating a homogenous mix. During sonication, the solution reached a temperature of 73 °C. A T18 UltraTurrax Homogenizer (IKA probe) was used to reduce particle size of hydrolysate in later studies and similar increases in temperatures were also seen. The probe was operated in a diluted volume of

hydrolysate (300 mL in a 600 mL beaker). To be consistent in this particle size reduction, this homogenization was conducted in the same beaker and geometry. Homogenization was carried out for 15 minutes total at 15000 rpm in order to mimic the effects of a high shear microfluidizer, which was not available in our lab (Jong, 2013).

1.2.4.2 Cellulose Dissolution Protocol (Side Study)

Cellulose dissolution was investigated as a method to dissolve and regenerate cellulose fibers and sclereid structures by immersion in a 7 wt% NaOH, 12 wt% urea aqueous solution, which was first precooled in a freezer (Cai et al., 2007). This solution was dripped onto microscope plates with solid suspensions of the soybean hull hydrolysate to view any degradation or gelation with the NaOH/urea solution and viewed under microscope at 100x, 200x, and 400x magnification (Cai & Zhang, 2006).

1.2.5 Analytical Methods

1.2.5.1 Dynamic Laser Scattering

Particle size analysis was done using a Wyatt Mobius Particle Size Analyzer (Wyatt Technology, Santa Barbara, CA). This device was able to detect particles up to 200 µm. Thus, the hydrolysate was diluted 100 – 1000 times to achieve a clean signal and avoid a concentrated sample. This sample was pipetted into a four-sided cuvette (important for letting the laser to hit the particles

90 degrees). Each measurement was averaged across five acquisitions and each sample was replicated by resuspending the dilution with a pipette to avoid the settling of smaller particles.

The hydrolysate was centrifuged even further, and the supernatant was tested to see how these solids would pack together. The resulting values from the instrument gave values in percent intensity, number, and volume. Because these were normalized values, it offered no information about absolute particle counts and gave relative percentages and distributions. Particle size analysis was done using a Wyatt Mobius Particle Size Analyzer. After centrifuging samples at 300, 1000, or 10000 rpm at various times the supernatant was diluted 100-1000 times. This sample was pipetted into a four-sided cuvette, which was important for letting the laser to hit the particles 90 degrees. Each measurement was averaged across five acquisitions and each sample was replicated by resuspending the dilution with a pipette to avoid the settling of smaller particles.

1.2.5.2 Scanning Electron Microscope (SEM)

A Hitachi-SEM TM3030 (Hitachi High-Tech America, Schaumburg, IL) was used to analyze the particle size of dried hydrolysate, and even to study dispersion in the rubber matrix. This was used primarily to study the shape of the dried nano- and micro-particles and to understand dispersion in the solid state.

1.2.5.3 Enzyme Analysis

For enzyme hydrolysis, the broth was thawed and centrifuged to isolate enzyme-rich supernatant. Each enzyme broth sample tested with its supernatant (diluted anywhere from 10 to 1000 times) using a blank, enzyme solution with substrate, and a blank with the enzyme substrate alone. These are all used to find the true signal from the enzyme-substrate complex in this colorimetric assay. For most of the protocols, the solution is first incubated in a water bath for varying times (depending on the enzyme of interest). Some of the assays require 5 mL DNS solution addition after incubation and diluted to test tube volume 25 mL with DI water and boiling for 10 minutes. The resulting colored complex is assayed for spectrophotometric absorbance values (optimally between 0.2-1.2). The enzyme activity, in U/mL (and FPU/mL for cellulase), was back-calculated with calibration curves developed by the Ju group. (Li et al., 2020).

1.3 Results

1.3.1 Fermentation Results

1.3.1.1 Submerged Fermentation of *A. niger* for Enzyme Production

Enzyme production was manipulated with pH control. This was previously studied in Li et al. (2020), where *A. niger* was studied for fermentation in four runs at different starting pH. The low cellulase activities, and high xylanase, pectinase, and α-galactosidase activities were consistent with previous results from the Ju group (Li et al., 2020). Below is the graph of one particular

fermentation run, showing the low cellulase production relative to the relatively high activities of pectinase, α-galactosidase, sucrase. pH changes over time are also shown in the graph below.

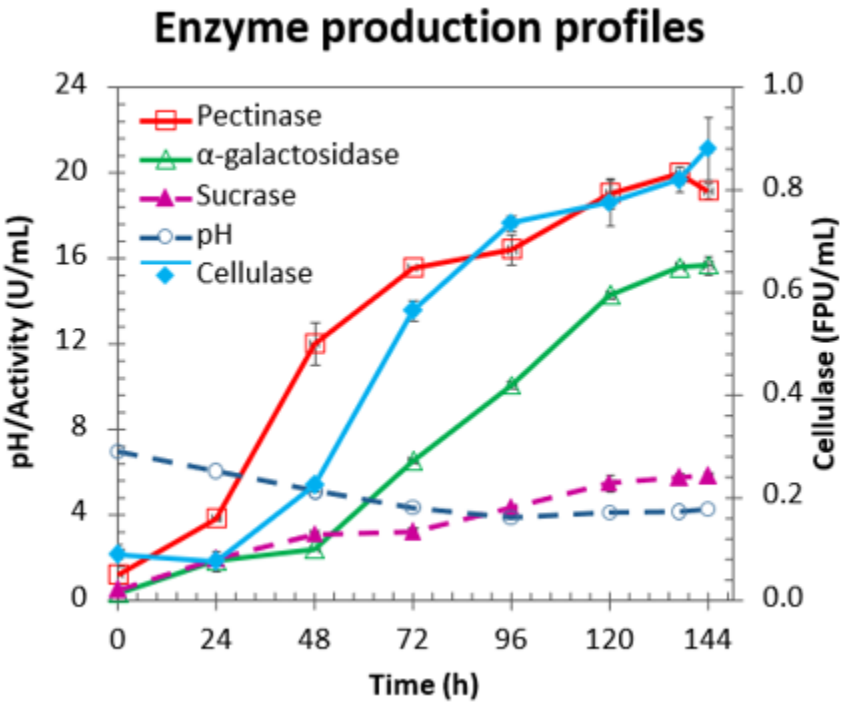

Figure 1-4. This plot shows the general trend of the enzyme activities [U/mL] and pH during fermentation of *Aspergillus niger*. The left axis is pH and the right axis is enzyme activity [U/mL].

The graph above details how the mycelium was able to sustain itself with the available biomass initially. The fungus grows on the biomass first and produces enzymes. These enzymes further breakdown the soybean hull into sugars and proteins that are soluble in the media, and thus easier to access as nutrients. This breakdown of biomass by enzymes creates a feedback loop of consumption. Additionally, because the enzymes themselves are composed of

nitrogen-rich amino-acid chains, they are also a nutrient source when *A. niger* is stressed for nutrients. This loop leads to fluctuating enzyme activity profiles as seen in Figure 1-4. The key takeaways from Figure 1-4 are that in these fermentations, the cellulase activity tends to be below 2 FPU/mL. Other enzymes critical for breaking down hemicellulose, namely xylanase, pectinase and α-galactosidase, exist in much higher concentrations ranging from 12-20 U/mL. (Li et al., 2020). These concentrations vary among fermentation runs and the final fermentation activity is used in subsequent hydrolysis design.

Dry solids were tracked for the fermentation run AN13 along with total carbohydrate content analysis. The 23.01 ± 0.12 g soybean hull loaded initially ended up resulting in a 5.80 (± 0.01) g unconsumed solids (25.2%) at fermentation end. In the supernatant, the total carbohydrates were found to be 2.346 g (10.2%) and other unsettled solids in the supernatant (soluble proteins or solids on the nanoscale and microscale) were calculated to be 14.87 g.

1.3.1.2 Observing Two Fungal Strains for pH Change Over Time

Two strains of fungus, *A. niger* NRRL 322 and *Scopulariopsis brevicaulis*., were inoculated and tested in a shakeflask. The pH was tracked over the course of two weeks.

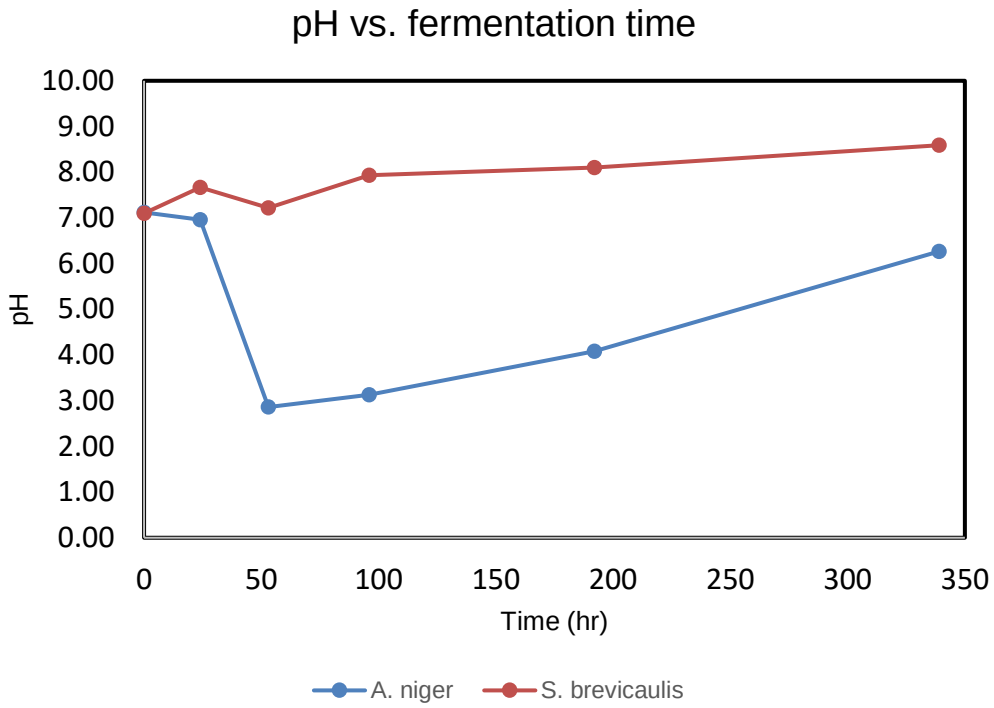

Figure 1-5. Two fungal strains (*A. niger*, *S. brevicaulis*) were compared for studying the degradation of sclereid compounds (discussed later in the enzyme hydrolysis section).

Measuring pH over the course of 350 hours (2 weeks) showed a pH drop for *A. niger* to pH 3 and a steady increase to pH 6. *S. brevicaulis* fluctuated between pH 7 and pH 8 for the initial 48 hours, but then plateaued at pH 8.

1.3.2 Enzyme Hydrolysis Results

1.3.2.1 Initial Enzyme Hydrolysis with Soybean Flour and Soybean Hull

Preliminary hydrolysis experiments were performed with soybean flour because this system was better studied by our lab. Below is the hydrolysis profile that was usually obtained after analyzing reduced sugars over time with HPLC.

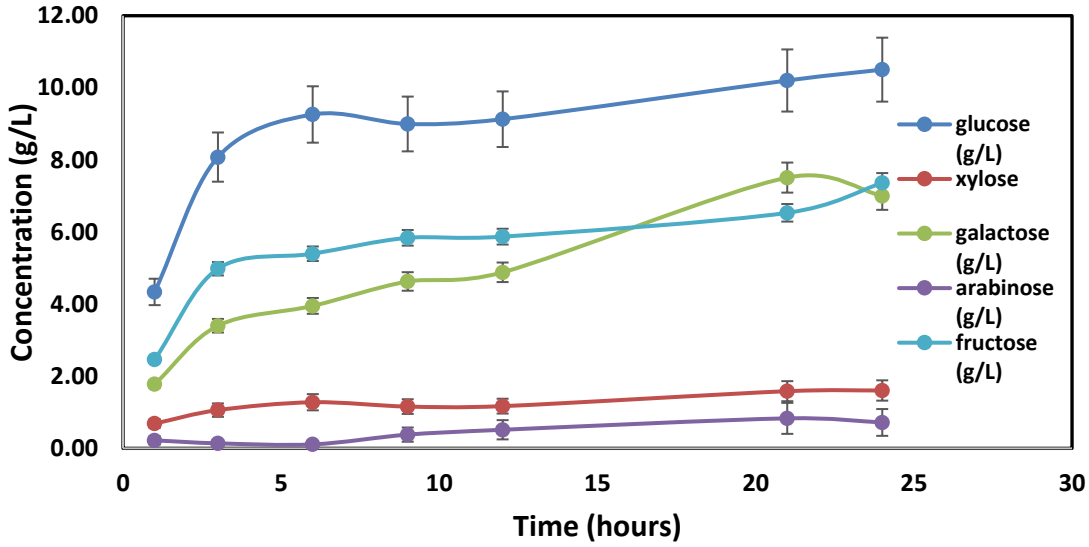

Figure 1-6. Time profile of sugar generation during enzyme hydrolysis of soy flour.

Reduced sugars were tracked with HPLC sampling. This graph shows that glucose was generated earlier in the hydrolysis and began to plateau between 12 to 24 hours after loading the shaker.

Enzyme hydrolysis was conducted at 2 FPU/g (a low level of cellulase loading). As mentioned in the Methods section under hydrolysis design, this design parameter was used with the prior knowledge that soybean hull contains

35.7% cellulose. Soybean hull and soybean flour loading was fixed at 100 g/L, based on previous experiments in this area (Loman et al., 2017).

Fixing the soybean hull loading allowed the cellulose content to be estimated. The cellulase activity (in FPU/mL) was obtained from the final fermentation sample. The volume of enzyme broth was calculated by using the known activity value in FPU/mL and the estimated cellulose content (g) such that the cellulase (on a weight basis) reached the design parameter of 2 FPU/g.

1.3.2.2 Soybean Hull Enzyme Hydrolysis at Nine Different Particle Sizes

An experiment was conducted in 50 mL centrifuge tubes to determine if starting particle size of ground soybean hull, sieved into nine different particle size distributions had an effect on sugar release. The resulting sugar content of glucose and the total mono-sugar release are presented in Table 1 after 24 hours of hydrolysis. Total sugar content ignored oligosaccharides that eluted at earlier run times in the HPLC chromatogram and total sugar content was calculated as the summation of reduced sugar concentration from cellulose and hemicellulose. Each particle size level was replicated with two centrifuge tubes. All tubes were loaded with enzyme broth at 2 FPU/g, as 10 FPU/g (recommended from previous studies) was too high and required five times as much enzyme volume. The enzyme broth from fermentation AN13 was used for this enzyme hydrolysis study. The enzyme broth in this study contained activities of xylanase at 2.253 (± 0.347) U/mL, and cellulase at 0.253 (± 0.019) FPU/mL. The activities of the other carbohydrases, sucrase, pectinase, and α-galactosidase were not available in

the datasheet for this run. Approximately two grams of soybean hull of each particle size was loaded into a 20 mL total hydrolysis volume. The results are shown in Figure 1-7 and Table 1-1.

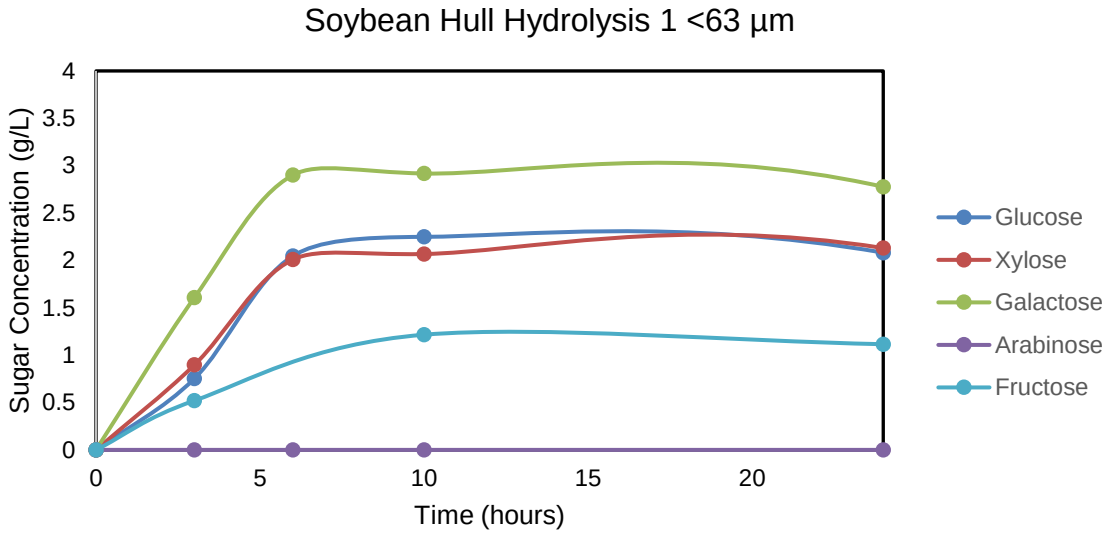

Figure 1-7. Time profile of sugar release during soybean hull hydrolysis (<63 µm).

Table 1-1. Glucose and total monosugar content after 24 hours-nine particle sizes.

Hydrolysis #	Particle Size Loading	Glucose (g/L) 24h	Total Reduced Sugar Content 24h
1	< 63 m	3.61 ± 0.36	14.33 ± 1.01
2	63 – 90	1.97 ± 0.24	10.39 ± 1.19
3	90-125	1.71 ± 0.51	7.87 ± 1.15
4	125-180	1.65 ± 0.32	6.07 ± 0.42
5	180-355	1.38 ± 0.55	8.35 ± 1.80
6	355-600	1.35 ± 0.02	4.86 ± 0.38
7	600-850	1.38 ± 0.01	6.59 ± 0.96
8	850-1180	1.23 ± 0.22	6.26 ± 0.51
9	>1180	1.07 ± 0.42	6.85 ± 1.03

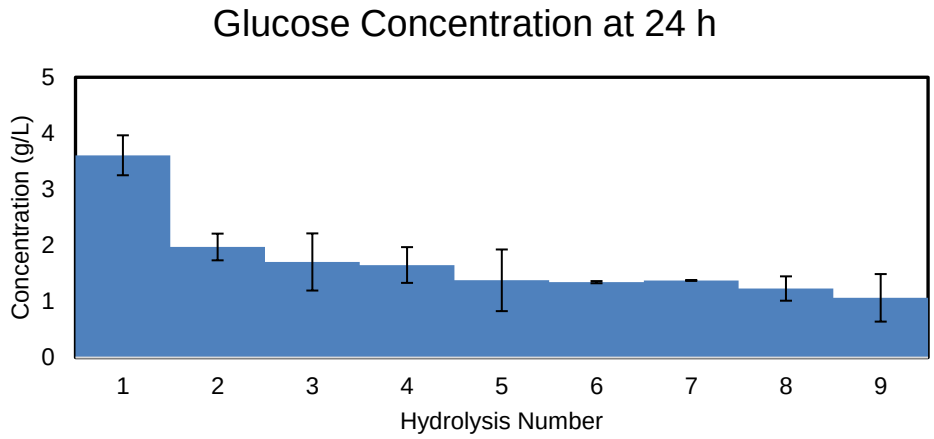

Figure 1-8. Glucose concentration after 24 hours of enzyme hydrolysis.

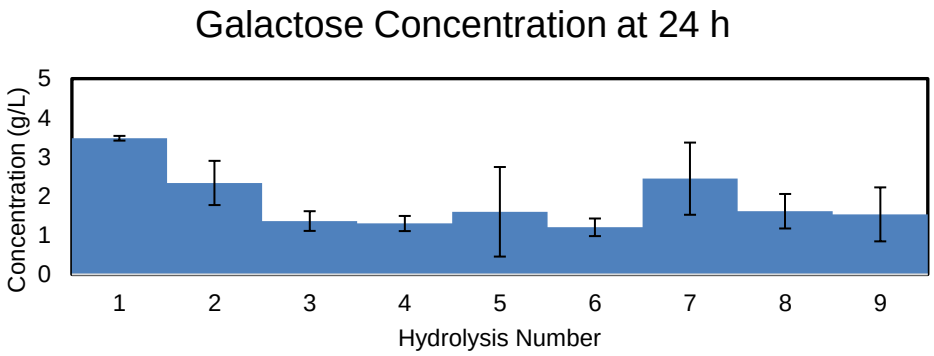

Figure 1-9. Galactose concentration after 24 hours of enzyme hydrolysis.

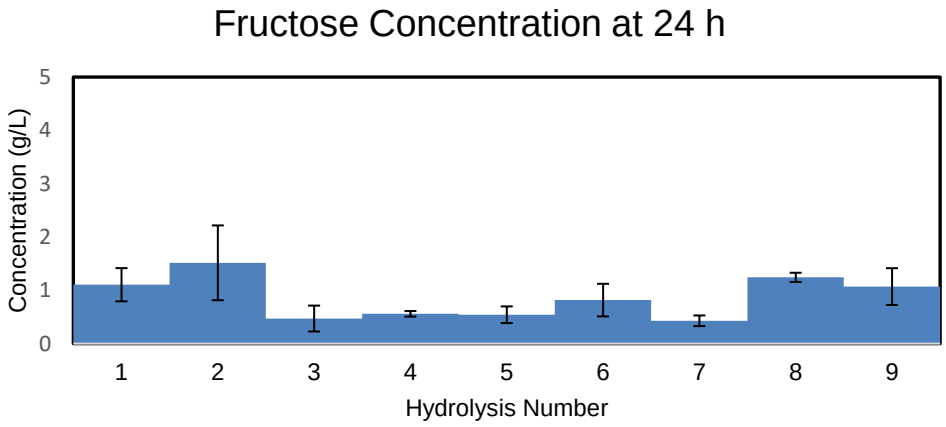

Figure 1-10. Fructose Concentration after 24 hours of enzyme hydrolysis.

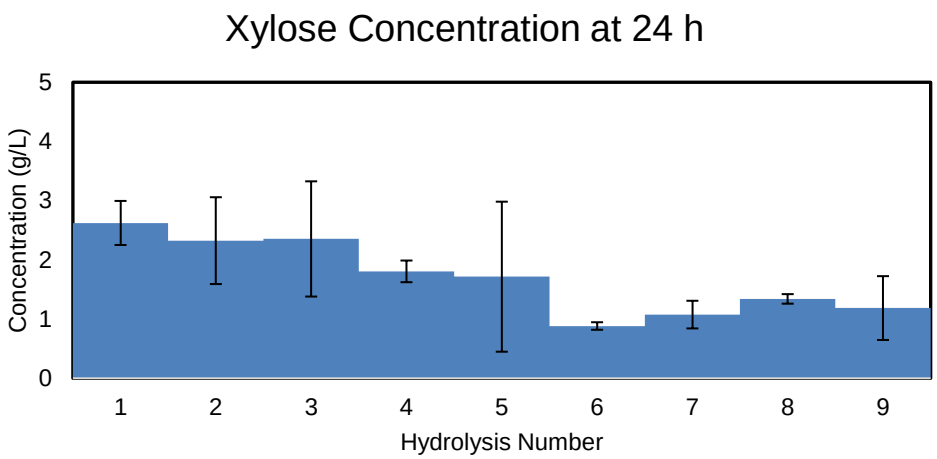

Figure 1-11. Xylose concentration after 24 hours of enzyme hydrolysis.

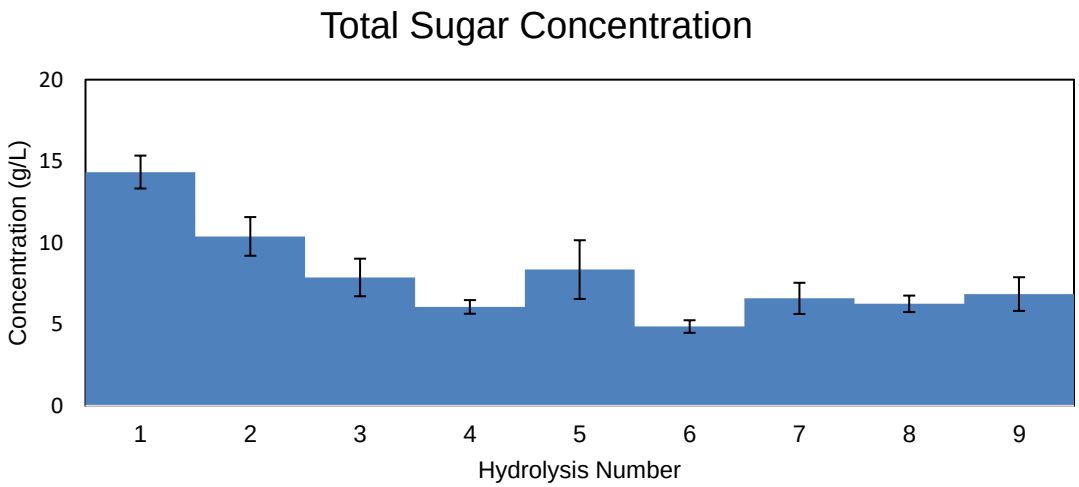

Figure 1-12. Total reduced sugar concentration after 24 hours of enzyme hydrolysis.

The smallest particle size (< 63 µm) generated a total monomeric sugar concentration of 14.33 (± 1.01) g/L and the largest particle size (> 1180 µm) generated 6.85 (±1.03) g/L in total monomeric sugar released after 24 hours. Upon looking at the glucose concentration at different particle sizes after 24 hours, there was certainly a trend showing that smaller particle sizes contributed

to greater glucose release. Some of the intermediate particle size ranges, namely 63 – 90 µm and 180 – 355 µm, generated total monomeric sugar concentrations of 18.58 (± 0.47) g/L and 18.40 (± 0.48) g/L, respectively. Furthermore, the error shown in these measurements reflects the HPLC chromatogram analysis and integration. Samples taken for HPLC were also viewed under microscope as a slurry prior to centrifugation for the supernatant. Figure 1-13 below shows how macrosclereid structures were progressively detached from the soybean seed coat during enzyme hydrolysis.

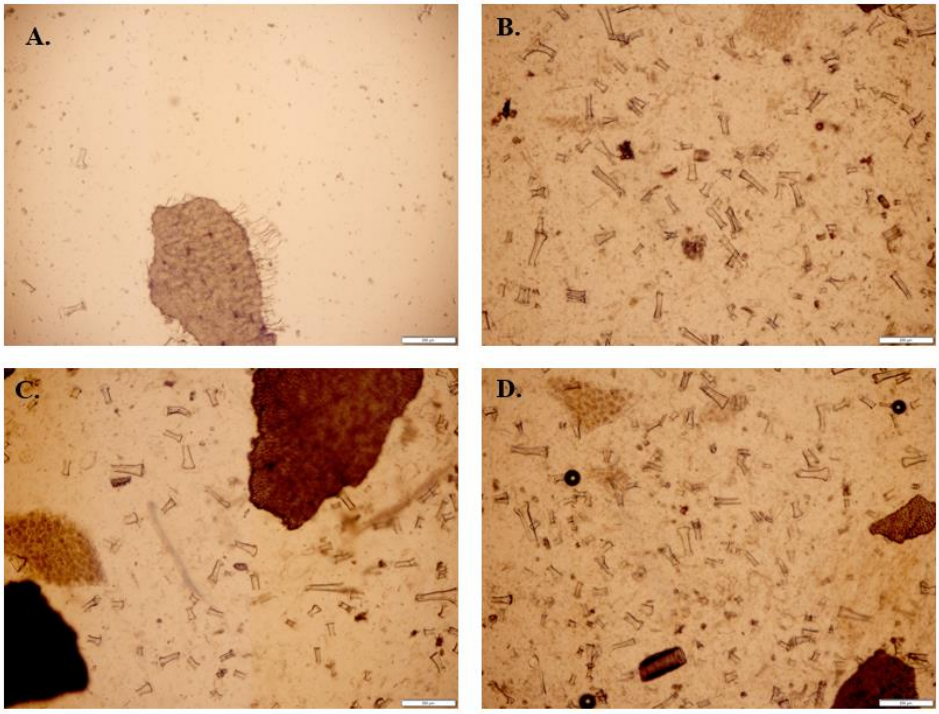

Figure 1-13. Compound microscope pictures showed how columnar, bar-like macrosclereids attached to the seed coat at the start of hydrolysis (A), are detached 7 hours later (B) and are seen in abundance at 12 hours (C) and 24 hours (D) for the particle size range 850-1180 µm (hydrolysis 8).

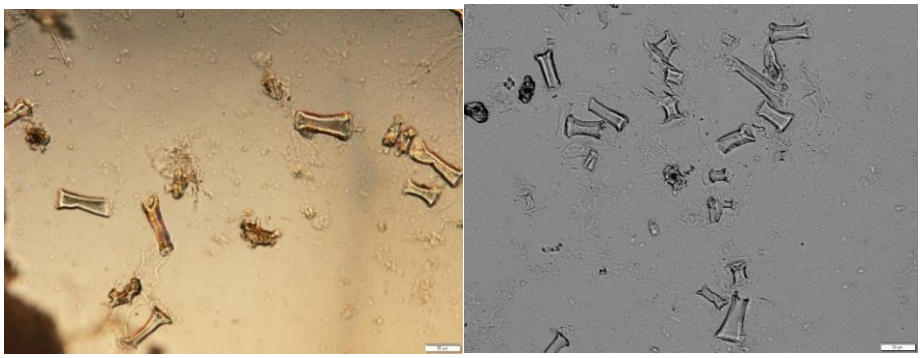

Figure 1-14. Hydrolysate 8 (850-1180 µm) showed the presence of these macrosclereids isolated from the soy hull structure surrounded by smaller particles in the background. After separating the sugars using centrifugation, the resuspended solids were viewed under grayscale.

The pictures in Figure 1-14 show the presence of ranges of particle sizes from 20-50 µm to 100-200 µm according to the scale in the image. In the background surrounding the sclereid structures smaller particles between 1 – 5 µm are visible, and this is supported from the particle size analysis results presented in the following sections.

1.3.3 Centrifugation and Size Analysis of Soybean Hull Hydrolysate

1.3.3.1 Centrifugation Studies for Dry Weight

Centrifugation time was also evaluated for two hydrolysate samples of different size ranges to study whether or not increasing centrifugation time from 10 minutes to 30 minutes increased the amount of solids settling out. Minimizing centrifugation time in the overall process would thereby reduce energy use if this process was to be scaled up.

Table 1-2. Centrifugation of soybean hydrolysates with two different starting particle size ranges to determine if longer centrifugation time at 10000 rpm resulted in major solid loss.

Hydrolysis Sample	Centrifuge Time [min]	Dry weight solids fraction [g]	% Increase
Size 1 (<63 µm)	10	0.0527	1.992
Size 1 (<63 µm)	30	0.0538	
Size 4 (125-180 µm)	10	0.0104	0.481
Size 4 (125-180 µm)	30	0.0103	

This study showed increasing centrifugation time to 30 minutes helped the packing/settling of solids increase by 2%, which was not a large increase to warrant increasing centrifugation time in later studies. Thus, centrifugation at 10000 rpm for 10 minutes was fixed for the washing of hydrolysates. Next, the amount of solids below 254 micron were studied using a stainless steel mesh to separate the particles. The filtrate through this mesh was also analyzed for soluble/non-settling components after centrifugation. A mass balance study was done with the hydrolysates with various particle size loadings to study how well recovery of small particles was after hydrolysis, and after mechanical treatments such as blending and vortexing. Mass percent was used here in an attempt to quantify the true amount of nanoparticles and microparticles in the system. It was later found that this mass percentage estimation may have been erroneous, and therefore the values were not reliable.

Table 1-3. Particle size and mass percent in the supernatant of hydrolysate solid suspension after 1000 times dilution.

Sample	Peak Diameters (nm)	Mass (%)
15 min 10000 rpm	41.3 ± 9.1	16.3 ± 3.7
	192.5 ± 11.8	82.1 ± 4.4
	65449.7 ± 15063.6	2.2 ± 0.3
30 min 10000 rpm	22.3	6.2
	163.8 ± 11.1	96.8 ± 2.7
	1725.5	4.6
	30209.7	2.2
45 min 10000 rpm	39.1	17.2
	164.1 ± 6.7	93.0 ± 7.8
	4932.4 ± 813.7	1.6 ± 0.5
	49766.2 ± 49739.6	2.5 ± 0.3
	182291.9	1.0
60 min 10000 rpm	24.5	8.6
	168.5 ± 9.5	95.2 ± 5.2
	2020.8	1.8
	29786.3 ± 9883.6	3.5 ± 0.3

1.3.4 Particle Size Reduction and Separation of Soybean Hull Hydrolysate

Sonication, blending, and homogenization were compared as techniques to reduce particle size of the soybean hull and soybean flour after enzyme hydrolysis. After centrifuging soluble sugars away from the hydrolysate after enzyme hydrolysis, the washed solids were resuspended in water and subject to mechanical disintegration. The disintegrated solid suspensions were tested for particle size analysis with DLS.

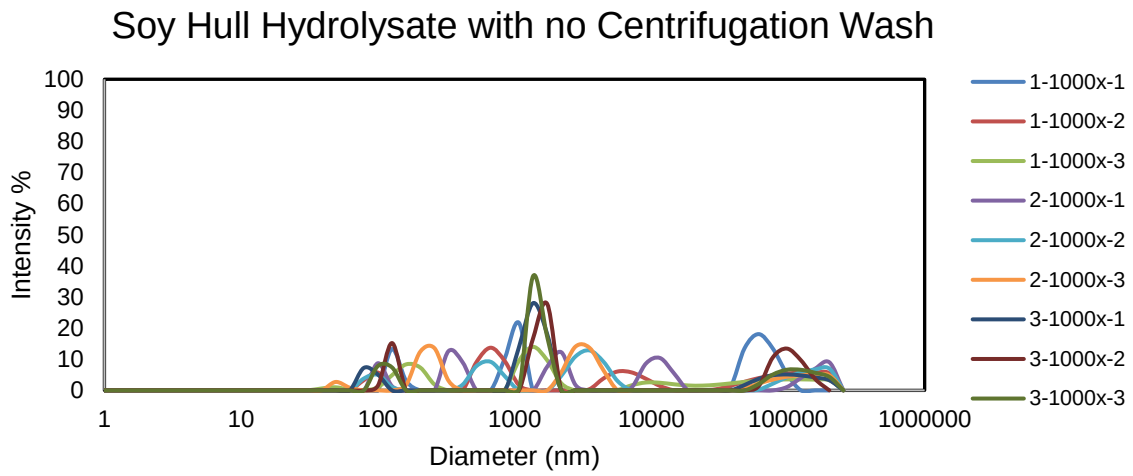

Figure 1-15. Particle size distribution for soy hull hydrolysate unwashed, uncentrifuged, and unfiltered at 1000x dilution.

At 1000x dilution, the soybean hull hydrolysate sample shows a wide range of particle sizes up until the detection limit of 200 micrometer. These results showed that there were three ranges below 200 µm that were able to be detected: (1) 50 – 200 nm, (2) 500 nm – 2000 nm (2 µm), (3) 20 – 150 µm. The microscope photos showed that there were still seed coat fragments and sclereid structures larger than 200 µm although the concentration of these particles was difficult to track.

1.3.4.1 Soybean Hull Sonication

Soybean Hull sonication increased temperature greatly and was ineffective in stirring created a viscous slurry that difficult to stir effectively and uniformly reduce particles temperature went up to 70 ºC. Sonication also had a limit, increased temperature of the hydrolysates slurry and was deemed

ineffective after 15-30 minutes. This process was difficult because it required intermittent sonication and used high energy (180 kW) and generated unfavorable noise. In the context of scaling up this process, sonication was slow and energetically unfavorable, and resulted in a small yield of filtrate and a massive filter cake.

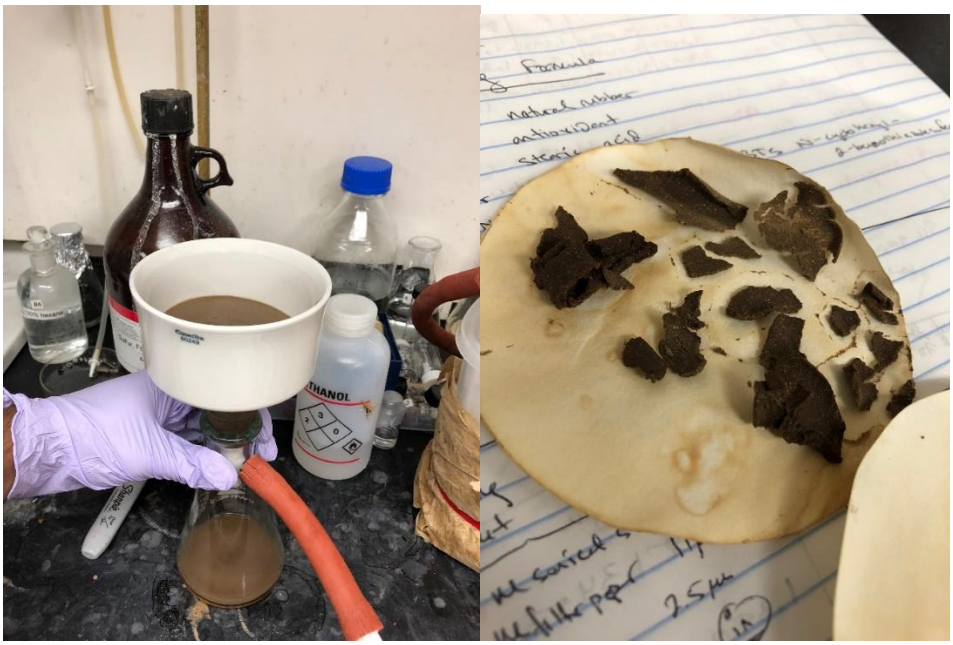

Figure 1-16. After sonication, the soy hull slurry was vacuum filtered through a 11 and 2.7 µm filter in two stages.

Figure 1-17. Film-like appearance of oven-dried filtrate (< 2.7 µm) after sonication.

Sonication was further studied with particle size analysis to understand the true generation of nanosized solids. Soybean hydrolysate was washed and resuspended in deionized water and sonicated at a constant power of 180 kW for 10, 20, and 30 minutes of cumulative sonication. Samples were taken at each time point and the centrifuged supernatant was diluted one thousand times and tested in the Wyatt Mobius to study how particle size distribution changed with increased sonication time.

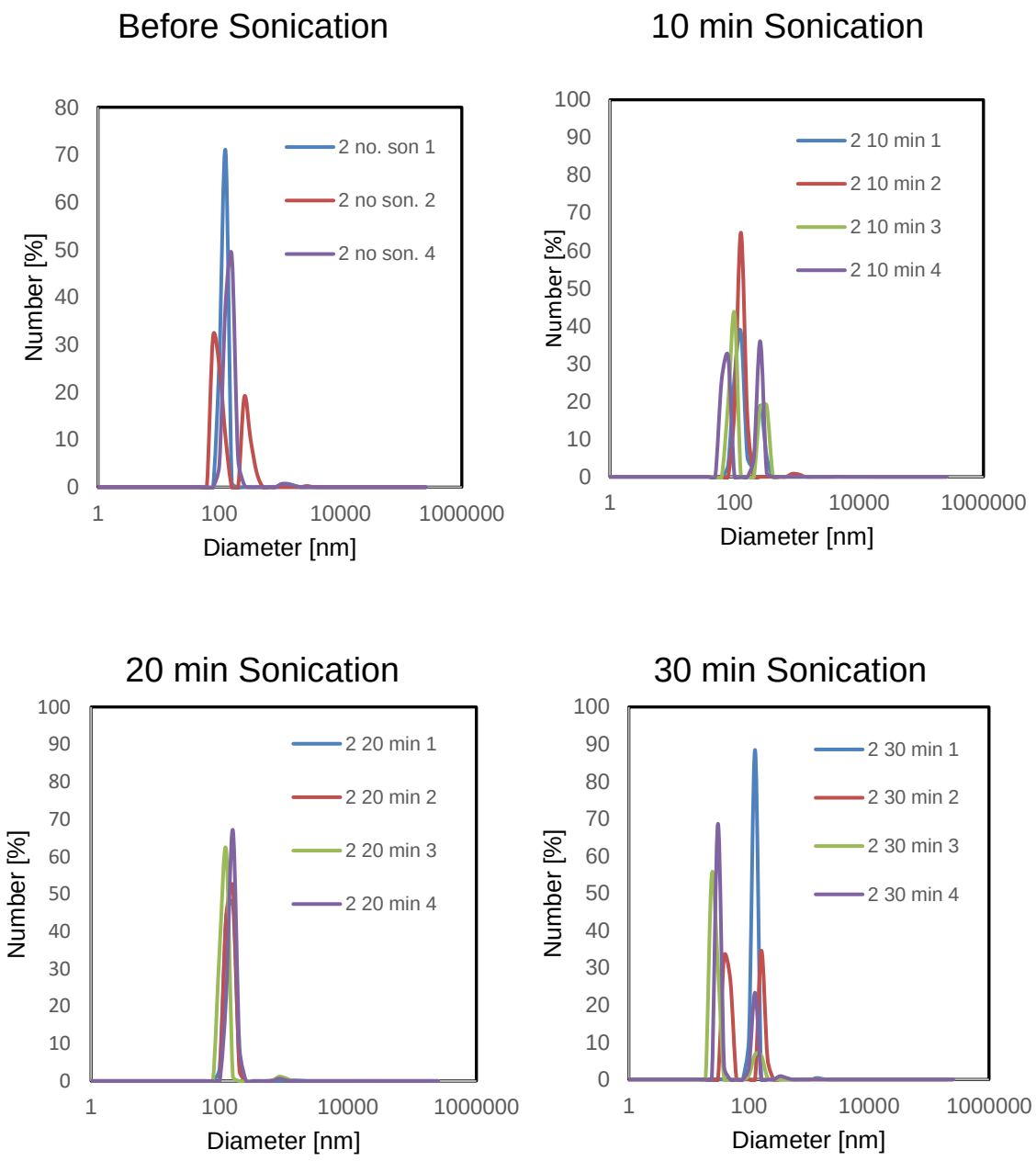

Figure 1-18. Results showing particle size distribution changing with increased sonication time (10, 20, and 30 minutes).

These results showed that insoluble nanoparticles were in the supernatant, and the lack of particles on the order of 1 micron and above suggested that size of particles most likely settled. Despite identifying the

presence of nanoparticles, the dry weight of this supernatant showed that these particles existed in such a small concentration that they would not be suitable for our downstream rubber processing in Chapter II.

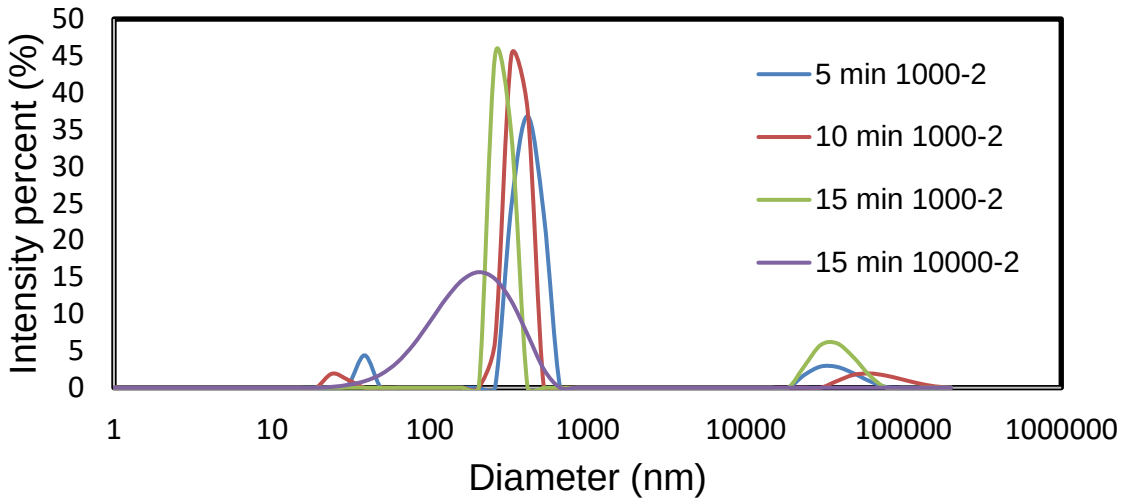

Figure 1-19. Particle size analysis of the soy hull supernatant after changing centrifugation speed and time.

This figure 1-19 shows how particle size distribution changed with two factors: centrifugation time and centrifugation speed. Centrifuging for a longer time showed peak shifting to the left, and centrifuging at higher rotor speed suggested that larger particles settle out allowing a wider distribution of smaller particles to be scattered by the laser. The meaning of these results mean that smaller particles are not spun down into the packed solids while particles beyond 1 micron appear to be settling after centrifuging for 15 minutes at the 10000 rpm. There were attempts made at separating homogenized solid suspensions with 2.7 µm and 11 µm filters. Filter cake formation was an issue that emerged when

vacuum filtration with these filter sizes was attempted. Filter cake formation prevented the desired nanoparticles from passing through the 2.7 µm filter. The largest measurable size for the particle size analyzer was 200 µm, thus any particles larger than that were not detected. There was difficulty in quantifying the exact mass percent of each particle size range for the resuspended soybean hull solids. The distributions were not completely reproducible in intensity and number percent, most likely due to settling effects over time and flocculation. The normalized percentages produced by the Wyatt Mobius made it more challenging to deduce the absolute count of the particles in each size range.

1.3.4.2 Soybean Hull Homogenization and Separation with Meshes

With the homogenized solid suspensions, another method to separate fractions of different sizes was attempted with steel meshes. However, the lack of a vacuum made this process very time consuming, as the slurry of these particle size distributions with meshes resulted in filter cake formation thus manipulating the isolated amounts. The mass was attempted to be deduced using dry weight analysis of filtrate and separated cakes.

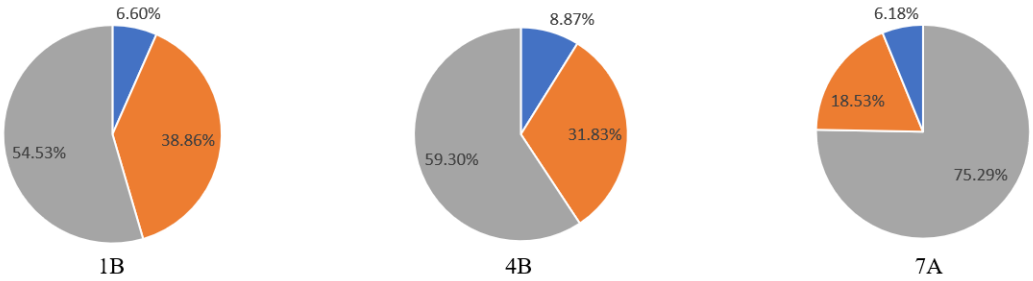

Figure 1-20. Fractional recovery of soluble components and solids smaller than 254 µm for three different starting particle sizes.

Mass balances were tracked from screening through a 254 µm mesh with three samples from the previous enzyme hydrolysis study at different particle size loadings: 1B (<63 µm), 4B (125-180 µm), and 7A (600-850 µm). The solids that were screened out (gray), the solids in the filtrate that settled after centrifugation (blue), and the soluble components and unsettled particles in the filtrate after centrifugation (orange) are shown above. Sample 7A was also vortexed for 15 minutes to study if smaller particles might be released and loosened into the medium. As expected, a majority of the solids larger than 254 µm were screened out in sample 7A. This showed that the efficiency of size reduction through enzyme hydrolysis was certainly correlated to the starting particle size of the soybean hull and that large particles were not sufficiently reduced in size with the enzyme loading used.

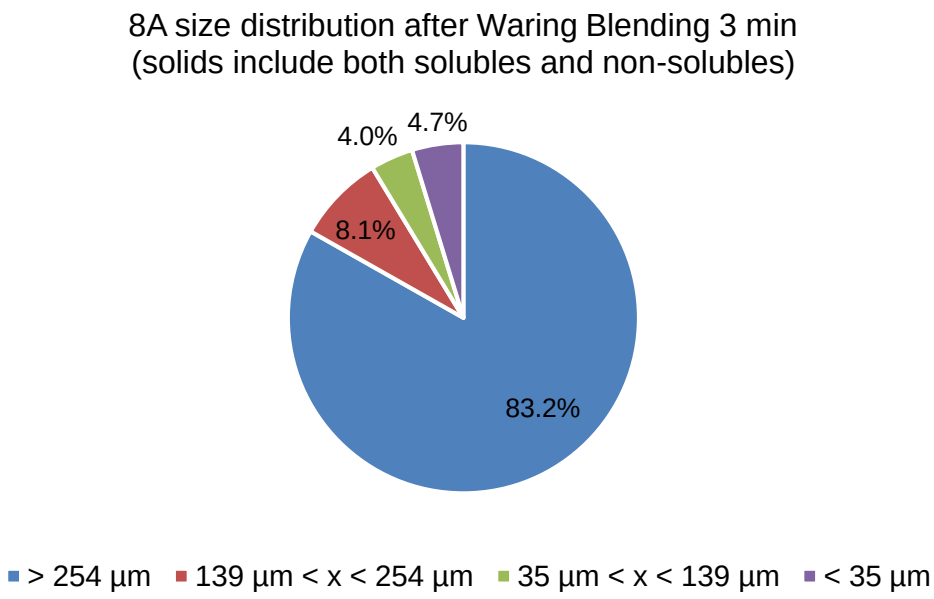

Figure 1-21. Fractional recovery of different particles size ranges after enzyme hydrolysis with a starting particle size range of 850 – 1180 µm.

A more careful mass balance study was done separating hydrolysate slurry with the starting particle size of 850 – 1180 µm. These results show that insoluble particles smaller than 35 µm are definitely generated through enzyme hydrolysis, but many of the solids above 254 µm are not sufficiently broken down by the enzyme at the 2 FPU/g cellulase activity tested.

In order to investigate how large these particles above 35 µm were, the hydrolysate slurry (without centrifugation) was diluted further and plated on a microscope to study the resulting structures. These results are shown in Figure 1-14 earlier, where bone-shaped sclereid structures approximately 200-250 µm in length were found. Additionally, seed coats untouched by the enzyme were also found in these microscope pictures.

1.3.4.3 SEM Pictures of Fermentation Broth and Soybean Hull Hydrolysate

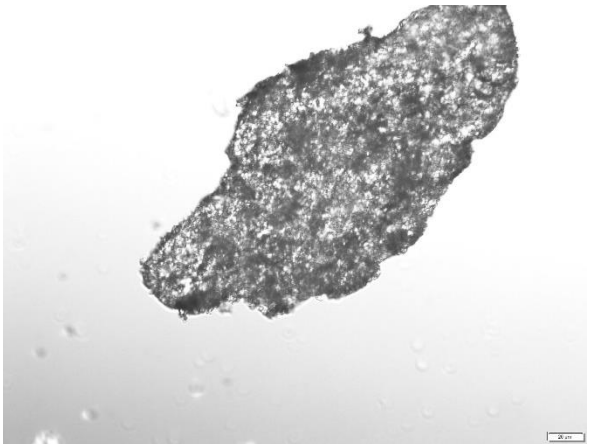

Figure 1-22. SEM image of soybean hull seedcoat before fermentation.

Prior to hydrolysis, the seed coat of the soybean hull was as pictured above. After fermentation with *A. niger*, the presence of bone-like sclereids as seen with a compound microscope, were also pictured under SEM. Strands and filaments, suspected to be either fibrils or remnants of mycelial growth, were also pictured with SEM.

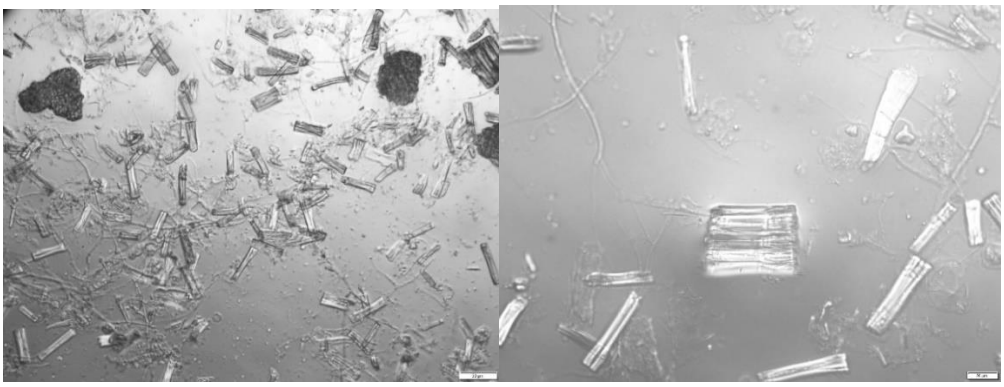

Figure 1-23. SEM pictures of the enzyme broth after fermentation showing the presence of bar like strutures, similar to what was observed under the microscope.

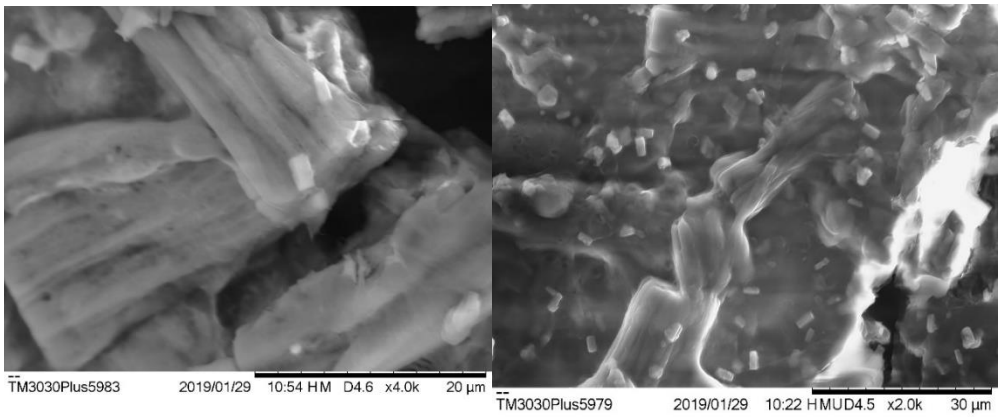

Figure 1-24. SEM picture of smaller particles on the surface of sclereid structures.

After enzyme hydrolysis with the enzyme cocktail, the soy hull hydrolysate was also imaged under SEM. The surface of the bone like structures appeared to contain even smaller particles within them. Macrofibrils were found to exist in these pictures with dimensions of 5-15 µm x 30-50 µm, as well as smaller particles with dimensions of 3 µm x 5 µm.

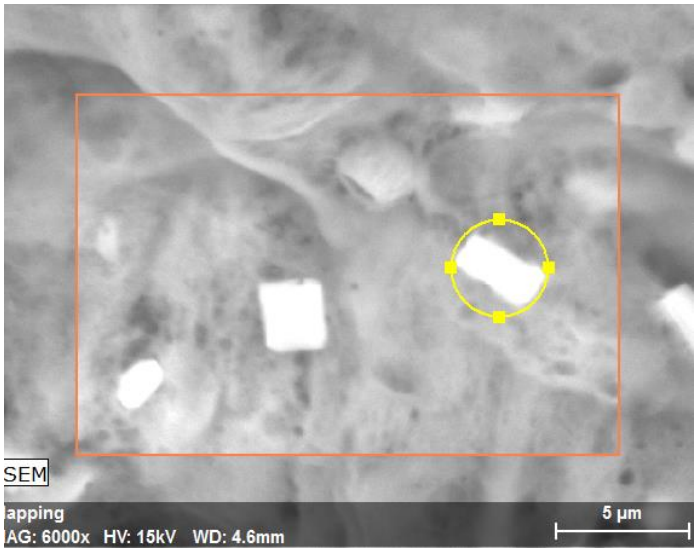

Figure 1-25. SEM picture of smaller particles on the surface of sclereid structures

The particles deposited on the surface of these sclereid structures appeared to be on the close to the nanoscale, and still attached to the sclereid structure.

1.4 Conclusions and Recommendations

1.4.1 Fermentation

Enzyme production was not entirely reproducible between fermentation runs, because SEM pictures from the fermentation broth showed fibrous particles on the microscale, with widths of 5-15 µm and lengths of 30-50 µm. There were also smaller particles with dimensions of approximately 3 µm x 5 µm in these SEM pictures seen deposited on some of the sclereid structures.

1.4.2 Enzyme Hydrolysis

Enzyme hydrolysis was initially conducted on a volume basis when initial experiments with soy flour and soybean hull were performed. These experiments were primarily done to understand when hydrolysis of the polysaccharides was mostly completed. These initial hydrolysates were used in preliminary rubber compounding studies in Chapter II, during which particle size reduction was not the primary experimental goal. The process of rubber drying downstream was the focus of these initial studies. Soybean flour was used over soybean hull due to the cleaner nature of the starting material, as soybean flour is further refined than the soybean hulls, which are separated earlier in the soybean refining process.

For the purpose of the overall process for downstream rubber compounding, minimization of glucose release was desired. For this reason, in the experiment with nine different particle sizes, enzyme loading was carefully designed on the basis of cellulase activity in the enzyme broth at 2 FPU per gram cellulose. When viewing under the microscope, this enzyme hydrolysis was found to isolate sclereids and macrosclereids from the hull structure.

When enzyme hydrolysis was conducted at 9 different particle sizes, there was a strong correlation between smaller particle size and total reduced sugar release. This finding agreed with the initial hypothesis that smaller particle size loading would result in easier enzymatic attack and greater sugar release. Because of this result, medium to large particle sizes (200 – 850 µm) were further studied for isolation of nanosized particles because of minimal sugar release of amorphous regions of cellulose.

When these hydrolysate samples of larger particle size were separated using steel meshes, the fraction of particles below 35 µm was found to be only 4.1%. After finding issues with separation, sonication, and blending, a homogenizer was next investigated to reduce particle size. Nanosized particles did exist in both the solids and liquid phases of hydrolysate. In order to minimize loss of nanoparticles, the soybean hull hydrolysate was washed after hydrolysis before mechanical treatment to remove enzymes and soluble components. The nanosized particles existed in small percentage relative to the particles between 25 – 50 µm and 100 – 200 µm, when the number percent of the particles was studied.

The resuspended soybean hull solution was subject to homogenization methods of sonication, homogenization, and blending. Blending was found to be a quick and effective alternative, but the particle size reduction was much less than sonication. The shear from the blending blades did not effectively reduce particle size and larger soybean hull structures, although it resulted in a more homogenous and particle size reduced solid suspension. There was not particle size data to support this claim, but upon viewing under a compound microscope large seed coast structures were seen intact. Blending and homogenization were not tested systematically with the particle size analyzer, as done in the sonication studies. Water loss and poor stirring were issues seen in sonication. It was postulated that the issue with stirring the slurry was related to the aggregation of small particles and loss of water from the medium.

1.4.3 Separation and Particle Size Reduction

In the soybean hull system, first sonication time was fixed and the particle size distribution of the supernatant after sonicating these resuspended solids for showed the presence of nanosized particles as small as 41.3 ± 9.1 and 192.5 ±11.8 nm and microparticles at 65.5 ± 15.1 μm after 15 minutes of centrifugation at 10000 rpm. Testing with longer centrifugation time continued to show that nanoparticles in the supernatant were detected at 22.3, 39.1, and 24.5 nm when centrifuged for 30, 45, and 60 min, respectively. On the basis of mass percent, the majority of these nanoparticles in the supernatant were detected at 192.5 (82.1%), 163.8 (96.8%), 164.1 (93.0%), and 168.5 (95.2%) nm for centrifugation

times of 15, 30, 45, 60 min centrifugation time, respectively. During this initial study of particle size reduction with sonication, it was realized that the mass percent reading was not an accurate estimate of the relative percentage of each size range. In the subsequent analysis, number percent was used as a better estimation rather than mass percent and intensity to correlate with the relative presence of each size range. When different sonication times (15, 30, 45, and 60 minutes) were tested, the resulting particle size distributions showed a widening of the curves. This indicated that more nanosized particles were being generated with increased sonication time.

In summary, for this set of sonication experiments of the soybean hull system it was learned that nanoparticles were indeed generated. The issue was primarily in learning how to effectively isolate these nanoparticles in a concentration significant enough for the second part of this project, the rubber processing. The bulk of the solids greater 200 μm were most likely settled in the solids fraction during centrifugation, and sonication was also deemed an energetically ineffective method to reduce particle size for the sample volume needed for later rubber processing (in Chapter II).

Sonication posed many problems with increased viscosity of the resulting sonicated solids. Furthermore, sonication seemed was energy intensive in this process and the sonication probe had a small working area and the effect of sonication was only localized near the probe – this became an issue when stirring was reduced, as the sonicator was only acting on a fraction of the solids.

Factors that were kept constant during this process were beaker geometry, sonication volume, stir bar used, and sonication time and power (180 kW).

The high shear microfluidization techniques employed by Dr. Lei Jong at USDA on soy protein isolate generated particles with diameters of 56 nm, which were much smaller that the size distribution achieved in our system (Jong, 2015). To mimic this microfluidizer, an UltraTurrax T18 homogenizer was used to disperse soybean hull solids. The probe allowed for easy dispersion and the same geometry and volume was used. After 15 minutes, the resulting slurry was subject to further screening and separation. As shown in the particle size results from before and after sonication, blending, and homogenization, the mechanical disintegration of the resuspended solids showed a widening distribution of particle sizes. This suggested that particle size reduction was successful at breaking down larger particles, such as the seed coats seen in previous microscope pictures.

Cellulose dissolution with a pre-cooled high pH sodium hydroxide and urea solution was found to be ineffective in breaking down macro and micro-sclereid structures. This may be partially related to poor mixing or the inability of sclereid structures to degrade easily. This experiment was a side study into how to breakdown insoluble solids that were not on the nanoscale.

1.4.4 Data Gaps and Recommendations

Due to the unforeseen circumstances of COVID-19, many planned side experiments and further investigation into using the homogenizer on soybean hull

solids were abandoned. A more thorough investigation of purifying nanocellulose and separating different particle sizes in a way to maximize throughput is necessary. It is recommended that more screening experiments with meshes and vacuum filtration have to be done in iterations, where screened solids have to be homogenized further and screened again. This process may avoid filter cakes that may trap nanoparticles. It is also recommended to experiment with commercial cellulase to break apart sclereid structures into nanoscale solids. The presence of nanocellulose can be further supported by FTIR spectra and better SEM photos to find out if CNFs have been successfully isolated. Running the isolated nanocellulose suspension through a mass spectrometer is needed to find the m/z ratio and confirm the presence of nanocellulose and different compounds. The HPLC of the resuspended soybean hull solids after washing away solubles should also be studied to see how much sugar remains trapped in the solids. The drying behavior of nanoparticles should also be studied to understand how they may behave when used in a composite, much like the rubber composites discussed in Chapter II. Particle size analysis should be reevaluated at different dilutions along with zeta potential in order to develop a better understanding of the nanosized particles in the system – it is recommended that this analysis is done with a DLS device that gives absolute counts of particles instead of the normalized percentage (number %, intensity %) that was seen in the Wyatt Mobius results. Although smaller particle sizes were found to generate more sugar and result in smaller solids recovery, the solids centrifuged from this process would be much easier to study in the particle size

analyzer and more focus could be directed towards actually obtaining cellulose nanofibers.

CHAPTER II

UTILIZING SOLIDS FROM SOYBEAN HYDROLYSIS AS A RUBBER FILLER

2.1 Introduction

2.1.1 Natural Rubber Background and Applications

Natural rubber is major commercial product from the previous two centuries and it comes from the sap of the Pará rubber tree *Hevea brasiliensis* (Malpighiales: Euphorbiaceae). Natural rubber is a polymeric fluid of varying chain lengths derived from the tree sap of *H. brasiliensis*. Natural rubber latex has been isolated from this tree and used for commercial purposes in South East Asia and Europe for the past 200 years, along with a long history of smaller uses in cultures of Mesoamerica, India, and South East Asia. Prior to the industrial boom of world war II, many of the uses for rubber were used for sports balls, gaskets, and concentrated latex (Rogers, 2016). Many uses of rubber revolved around the elasticity of rubber for these purposes. Natural rubber consists of various chain lengths of *cis*-polyisoprene, and when this sap is dried it produces an elastic and flexible solid, which is in high demand for various applications ranging from household products to vehicle tires. Natural rubber is best known for its versatile use in latex products and tire treads. The tapped latex is 30-35%

rubber, 60% aqueous serum, 5-10% fatty acids, amino acids, proteins, starches, sterols, esters and salts. For tire tread applications, the wear-and-tear nature of driving vehicles necessitates the use of fillers to reinforce these composites. (Rogers, 2016).

2.1.2 Filler Production and Rubber Applications

Major fillers in this process are currently silica and carbon black. Silica is derived two ways – through precipitation or fuming. Precipitated silica (SiO_2) is produced through sodium silicate and water and ion exchange and is widely used as an inorganic filler. Carbon black is produced by burning hydrocarbon fuels with limited air between 2400-2800 F^o and is conventionally produced two different ways – the oil furnace, and the thermal process. Despite carbon black being very affordable ($2400/ton) and of low density (ρ = 1.8 – 2.1 g/cm^3), this product is the result of an environmentally costly process because petrochemical products are used as the raw materials. Silica, despite being inorganic and less environmentally damaging, lacks the abrasive resistance carbon black provides for tire tread purposes (Wampler et al., 2016).

There is a major market need for composites of varying strengths for different end polymer applications, as well as stability and durability of the polymer composite. Conventional fillers used to reinforce polymer composites like carbon black and silica can also act as crosslinking agents, Recent advances in nanotechnology has motivated researchers to use reinforcers on the nano-scale for their high surface area and the ability to raise the modulus of a

composite, thus reducing elasticity and improving tensile strength of such composites. Dr. Lei Jong has previously succeeded in particle size reduction of soy protein isolate and soy protein powder and used them at different filler concentrations to reinforce natural rubber (Jong, 2017).

Rubber compounding is the act of using this tapped latex for industrial and commercial purposes (Rogers, 2016). Nearly 75% of natural rubber production is directed towards tires, the remainder for medical latex applications and other automotive fields. The latex drying process sometimes ranges from 5-7 days at 60°C and is done to increase viscosity of the resulting latex. A possible downside of using natural rubber is that it can harden during storage, due to the oxidation of polymer chain forming ketones and aldehydes, as well as shortening chain lengths. The oxidized aldehyde-chains react with proteins and result in a gelation (Rogers, 2016). In tire tread applications, natural rubber content ranges from 10 – 100 parts per hundred rubber (phr) (Rogers, 2016). Work has been done in recent decades to explore different rubber polymer combinations, such as polybutadiene, styrene-butadiene, to test combinations of rubber bases. Tire sidewalls, for example, contain 50% polybutadiene and 50% natural rubber. Reinforcing fillers with biotechnology sources (rice husks, starch, bamboo fibers, white rice husk ash) can improve rolling resistance if used with a silane coupling agent (Xie et al., 2010).

2.1.3 Rubber Compounding

Rubber compounding is a multi-step process to strengthen or plasticize the rubber product by adding chemical additives prior to curing. The process used in this work involves three major steps: (1) drying the natural rubber latex, (2) adding chemical additives and accelerators to reduce rubber viscosity, and (3) curing the rubber through sulfur vulcanization. Many general purpose elastomers use initiators such as full form (THF) and organolithium activators. (Colvin, 2016). There are two types of elastomers: thermoplastic and thermoset; thermoplastic elastomers can be molded, remelted, then reprocessed for other use (Colvin, 2016). Thermoset polymers are molded and remain permanently in a solid state. In the 1840s, Charles Goodyear discovered that vulcanizing, or cross-linking sulfur with rubber at a high pressure and temperature, resulted in a stronger, tougher rubber product (Ignatz-Hoover & To, 2016). This was key for preventing rubber from softening in heat (Abraham, 2016). The previous century prioritized ways to make these vulcanized products stronger through the use of reinforcing fillers discussed earlier, such as carbon black and silica (Wesley A. Wampler et al., 2016). These advances led to a refinement of the rubber-making process. Mixing generally uses powders and solid rubbers in an internal mixing mill to reduce viscosity, control heat generation, and incorporate and disperse fillers successfully. Other factors during this mixing step include homogenization, sticking release, and mix time (Moneypenny et al., 2016).

2.1.4 Rubber Vulcanization and Optimum Cure Time

After the composite is mixed in the mill, it is then vulcanized by compression, transfer, injection molding, or continuous vulcanization (Ignatz-Hoover & To, 2016). Studying vulcanization is important for understanding the scorch, flow, and component state of the cure. Vulcanization is a key process that occurs when rubber is heated to temperatures between 140 – 160 °C with sulfur, which results in a stronger, crosslinked rubber product. The chemical reaction that occurs during vulcanization is the breakup of sulfur into free radicals, allowing chains to polymerize with the natural rubber (*cis*-1,4-polyisoprene) (Ignatz-Hoover & To, 2016). Additionally, it is essential to study curative migration and dispersion, mold release, fouling, cleaning, and the surface appearance. To improve the dispersion of filler particles, the elastomer is first treated with chemicals to reduce plasticity, tackiness, and temperature sensitivity. The thermoplastic elastomer turns into a three-dimensional elastic network. Scorch is the initial formation of the network in rubber, and after scorch occurs the rubber cannot be further shaped or processed (Ignatz-Hoover & To, 2016). Scorch safety of the rubber and optimal cure time are important to study for this reason – the time to scorch is a critical parameter for curing the rubber compound effectively. The rate of cure, or the rate at which crosslinks form, dictate the optimum cure time, which is the time required to achieve 90% of maximum cure. The state of cure is also studied in immersion studies to deduce the degree of crosslinking, or crosslinking density. An accelerator is also used to aid in sulfur crosslinking to improve efficiency of curing. Optimal cure time is

studied using a moving die rheometer (MDR). MDR results for studying cure time of un-cured natural rubber after mastication in a Brabender mixer are displayed in Figure 2-1.

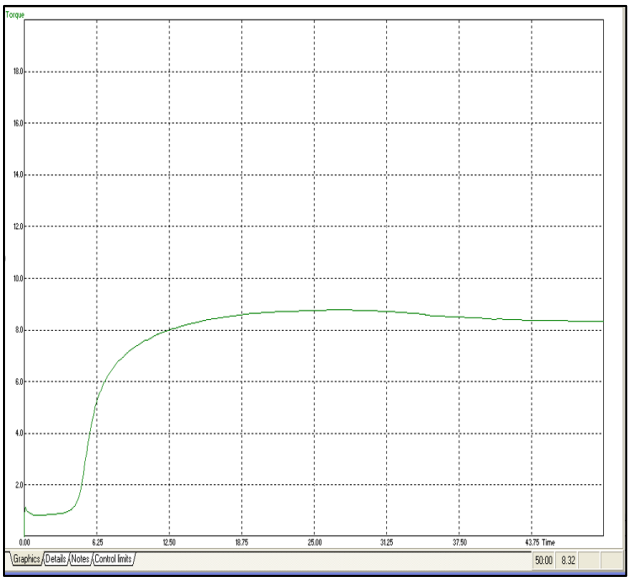

Figure 2-1. Moving die rheometer graph of uncured natural rubber. An initial dip in the beginning of this curve shows scorching and t90 is deemed as 90 percent of maximum torque.

The figure above shows that the natural rubber sample peaks in torque at 9 Nm. The mixing process helps in blending the polymers and fillers and reducing viscosity in order to achieve a homogenous solid mix and minimize the scorch time. Vulcanization is then used at high pressure and high temperature to create sulfur cross-links in the polymer-filler network and introduce adequate compound-compound adhesion, as well as releasing trapped air in the rubber introduced during mixing (Ignatz-Hoover & To, 2016). This process occurs

generally at high pressure, high temperature oven. In compression molding, the mixed rubber composite is placed between two platens and heated to 150 °C at pressures as high as 5 MPa for an optimal cure (Jong, 2017). Depending on the rubber used (different blends vs. pure natural rubber) the processing and additives may differ (Jong, 2018). Addition of reinforcing fillers poses problems related to filler dispersion. Furthermore, the conventional use of fillers in the processing of rubber composites use fillers that are either derived from environmentally harmful processes or produced so expensively that they cannot be scaled for industrial rubber processing. The following methods and results sections focus on utilizing the soybean solids after enzyme hydrolysis, separation, and mechanical treatment discussed in the previous chapter. In Chapter I, soybean hull and soybean flour were hydrolyzed with *A. niger* enzyme broth with varying carbohydrase activities. This hydrolyzed biomass suspension was washed to collect the solids that were not hydrolyzed by the enzyme and other soluble components (proteins, ash). These solids were later subject to mechanical treatment (blending, sonication, or homogenization) to reduce the particle size of the suspension. Although nanoscale was not achieved in Chapter I, the resulting biomass suspension was mixed with the natural rubber latex at alkaline pH (9.8-10) at 30 parts per hundred rubber (phr) and oven dried. The dried rubber was next rubber compounded, compression molded, and assessed with tensile testing and imaging.

2.2 Methods

2.2.1 Materials

Soybean hull and soybean flour were obtained from Archer Daniel Midlands company (Decatur, IL). Chemicals were purchased from Sigma Aldrich (St. Louis, MO). Natural rubber latex (CENTEX Latz) was obtained from Killian Latex, Inc. (Akron, OH). Carbon Black (CAS 1333-86-4) (VULCAN® M N339) was purchased from the Cabot Corporation (Billerica, MA). Carbon black was determined to have 39 nm diameter. A Brabender Plasticorder (75 cc REE6 Mixing Bowl, Banbury Blades, 40-80g capacity) and a TPM Compression Mold (Akron, OH) was used to vulcanize the rubber composite.

2.2.2 Rubber Drying

The mass of dried rubber (especially for the composites created with aqueous dispersions of the bio-based filler) was tracked to ensure the water was evaporated after overnight drying. The criteria for ending the drying process at 70 ºC was the water evaporating above 95% and no change <3% between consecutive measurements. Overnight drying at 70 ºC was followed with a few hours 100 ºC to eliminate all the water in the system. Mass balances were very critical to this rubber making process, as sufficient mass was needed for at least two moving die rheometer measurements and at least 45 g of the mixed rubber was needed for compression molding. Furthermore, the ideal loading of the Brabender Plasticorder was between 50 – 65 g (approximately 70% of mixer

volume) and loading beyond this limit created problems for rubber mastication and filler dispersion.

2.2.3 Compounding Protocol for Natural Rubber Composites

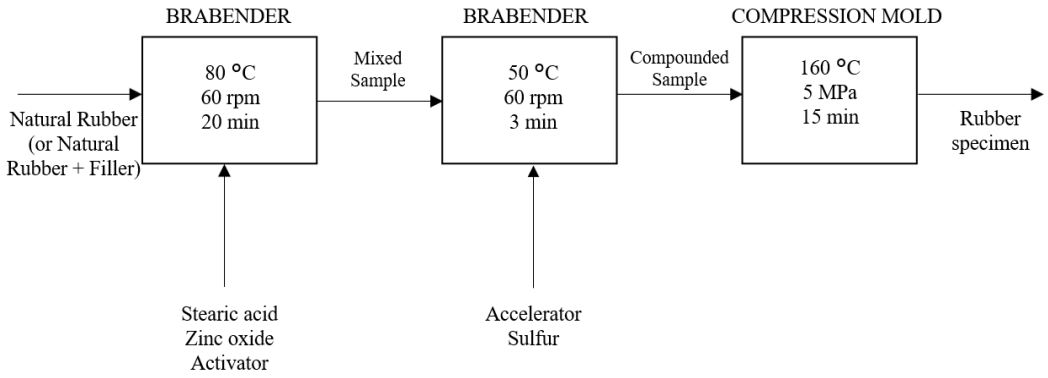

Figure 2-2. PFD of the rubber compounding with the inputs, temperatures and RPM requirements of the internal Brabender mixer.

This flow diagram is based on the methods Dr. Jong previously used in his soy-protein reinforced rubber composites (Jong, 2017). The main change in protocol is the addition of sulfur and accelerator; in this work sulfur and accelerator are added at 50 °C to avoid scorching. Additionally, a curing temperature of 150 ºC (instead of 160 ºC) was recommended from fellow polymer science students. The washed soy hull hydrolysate after blending or sonication was adjusted to pH 9.8. The mixture was then poured into a Waring Blender and blended for 1 minute to promote mixing, then deposited into a glass dish for drying overnight at 70 °C. The dried rubber was also subject to heat treatment for 4 hours at 100 °C. After drying, the sample was then compounded with the following formula with the dry rubber as the basis for parts per hundred

(phr) calculation. On a 100 phr dry rubber basis the additives used were 2 phr stearic acid, 5 phr zinc oxide, 1 phr 2,2'-methylenebis(6-tert-butyl-4-methylphenol), 2 phr CBTS N-cyclohexyl-2-benzothiazosulfenamide, and 2 phr sulfur. Zinc oxide, antioxidant, and stearic acid were first fed at 80 °C and forward internal rotation at 60 rpm. After 20 minutes of mixing, this rubber mass was removed and the mixer was cooled to 55 °C. The rubber was fed in once again along with the CBTS accelerator and sulfur for a total of 5 minutes (Jong, 2017).

2.2.4 Rubber Composite Curing

This masticated sample was removed from the mixer and subject to moving die rheometer measurements to find optimum curing time. A five gram sample was placed between blank mylar sheets and loaded between two platens. These platens were pressed together at 150 ºC and the resulting curve of torque (Nm) vs. time was generated over a 30-45 minute period until maximum cure and subsequent scorch was assessed. The average of two or more MDR measurements was used to determine optimal cure time t90 for the compression molding press. After determining the optimum curing time, t90, the samples were compression molded in a TPM Vacuum Compression Press at the University of Akron Olson Research Center. The samples were placed in the center of a 4.7" x 4.5" stainless steel mold at the optimum cure times (t90) at 5 MPa (approximately 15000 lb_f for the area of the mold) and 150 °C (Jong, 2017).

2.2.5 Rubber Composite Characterization

2.2.5.1 Tensile Testing

The resulting rubber samples were die cut in dumbbell (or dogbone) samples according to both ASTM D412 and D638. For ASTM D412, the extensometer gauge length was calibrated to 25 mm, and for ASTM D638 the extensometer gauge length was adjusted to 10 mm. ASTM D638 was used to die cut and test smaller samples when large areas were not available to die cut. The width of the samples varied from 3.0 – 3.3 mm, in accordance with the ASTM requirements. The test was conducted with an Instron Model 5567 (5567P5715) at the University of Akron. The crosshead speed during the test was fixed as 500 mm/min, and the stress-strain curves and elastic moduli at 100% and 300% elongation were obtained in BlueHill 3 software.

2.2.5.2 Rubber Swelling for Estimating Crosslinking Density

The gel swelling measurements were performed by immersing 2 grams of each rubber sample in 20 mL toluene. After immersing the rubber samples for 48 hours at room temperature, the swelled rubber was vacuum dried at 50 °C (Jong 2015). Crosslinking density was estimated with the following equation:

$$Crosslinked\ density = \frac{\Delta \mathrm{m}}{\mathrm{m}_{\mathrm{initial}}} * 100,$$

which gave an estimation of the percent crosslinking in the sample.

2.3 Results

2.3.1 Initial Rubber Composites

2.3.1.1 Initial Tensile Tests with Soy Molasses, Soy Flour Hydrolysate Fillers

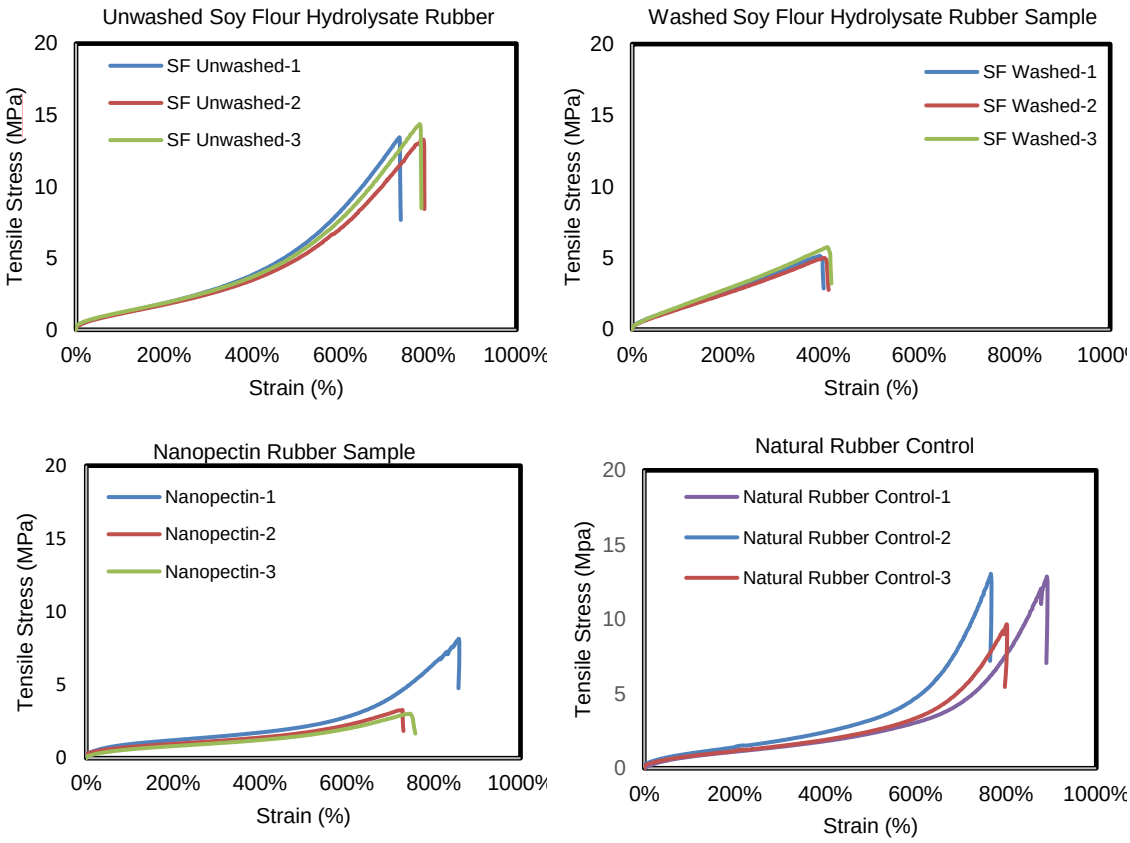

Figure 2-3. Stress-strain curves for initial soy flour hydrolysate-rubber composites. Clockwise from top left: (1) Soy flour hydrolysate (2) Soy flour hydrolysate after 1 wash (3) No filler, and (4) Nanopectin from soy molasses, centrifuged and washed four times.

2.3.1.2 Crosslinking Density for Initial Rubber Composites

Table 2-1. Crosslinking Density for Initial Rubber Composite Samples.

Sample	Approximate Crosslinking Density [%]
SF 1 wash	15.2 ± 2.4
SF unwashed	18.2 ± 1.0
Nanopectin	23.0 ± 1.3
NR	32.7 ± 4.2

Crosslinking was not tested for subsequent samples due to the high volume of toluene required for submerging and swelling the rubber sample, which would generate a large amount of organic waste. The crosslinking density varied from sample to sample likely because these samples were not yet cured at the optimal cure time.

2.3.1.3 Retesting of Soy Flour Hydrolysate Rubber Composites

Next, soy flour hydrolysate was compounded once more to test alongside natural rubber after the compounding and curing process was better understood.

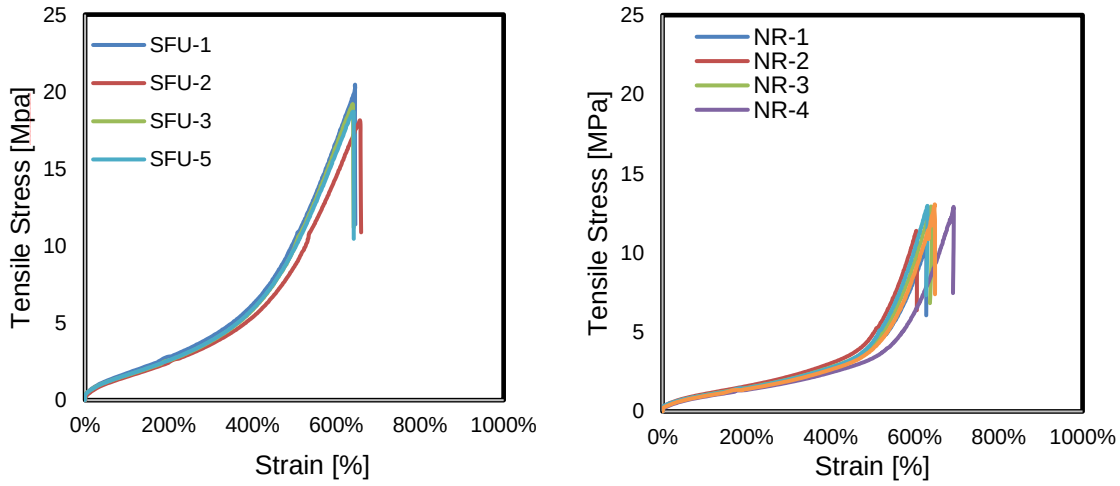

Figure 2-4. Retesting soy flour hydrolysate as a filler in natural rubber.

The table below shows the ultimate tensile strength and the elastic moduli for these rubber samples. These values were crosschecked with Dr. Jong's previous results for natural rubber to see if these values were within error of his values (Jong, 2018).

Table 2-2. Tensile Stress and Strain and Modulus at 100% and 300% Strain.

Sample	Max Stress (UTS) [MPa]	Tensile Strain at Break [%]	Tensile Stress at Break [MPa]	100% Modulus [MPa]	300% Modulus [MPa]
Natural Rubber	12.3 ± 1.1	641 ± 30	12.0 ± 1.1	1.0 ± 0.1	2.0 ± 0.1
Soy Flour Hydrolysate (30 phr)	19.1 ± 1.0	646 ± 8	19.0 ± 1.0	1.6 ± 0.1	3.8 ± 0.2
Natural Rubber (Jong, 2018)	13.2 ± 2.0	540 ± 17	13.2 ± 2.0	0.9 ± 0.1	2.4 ± 0.2

2.3.2 Rubber Compounding Results with D-Glucose as a Filler

A study was performed to assess the reinforcement effect of glucose in natural rubber. The natural rubber basis was kept constant at 40 grams, and four glucose concentrations (1.25, 5, 20, and 30 PHR). The glucose was dissolved in a constant volume of 120 mL water, mixed with natural rubber latex and oven-dried overnight.

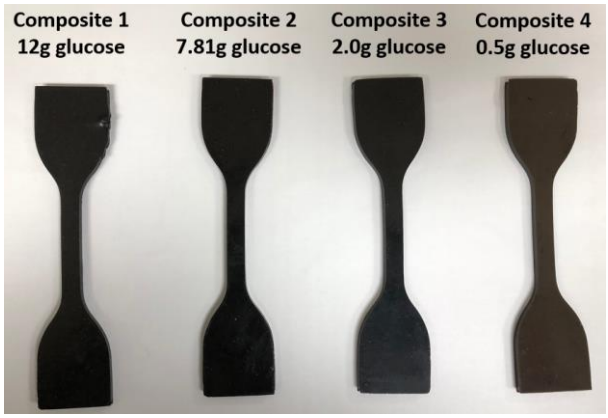

Figure 2-5. From left to right, composite 1 to composite 4 glucose-rubber samples.

2.3.2.1 Testing Results of Glucose-Rubber Composites

Table 2-3. The stress and strain at break and the elastic moduli from tensile testing glucose-rubber composites at four different filler loadings.

Sample	Tensile Strain at Break [%]	Tensile Stress at Break [MPa]	100% Modulus [kPa]	300% Modulus [kPa]
no filler 0 phr	251 ± 59	2.9 ± 0.8	1240 ± 18	-----
1.25 phr glucose (0.5 g)	512 ± 14	23.6 ± 2.1	1093 ± 34	3104 ± 146
5 phr glucose (2.0 g)	576 ± 12	18.6 ± 0.8	904 ± 13	2255 ± 81
20 phr glucose (7.8 g)	603 ± 16	9.9 ± 0.8	704 ± 21	1563 ± 74
30 phr glucose (12.0 g)	643 ± 34	10.4 ± 0.9	746 ± 48	1589 ± 80
30 phr carbon black	308 ± 21	22.3 ± 2.8	3223 ± 109	21457 ± 3776

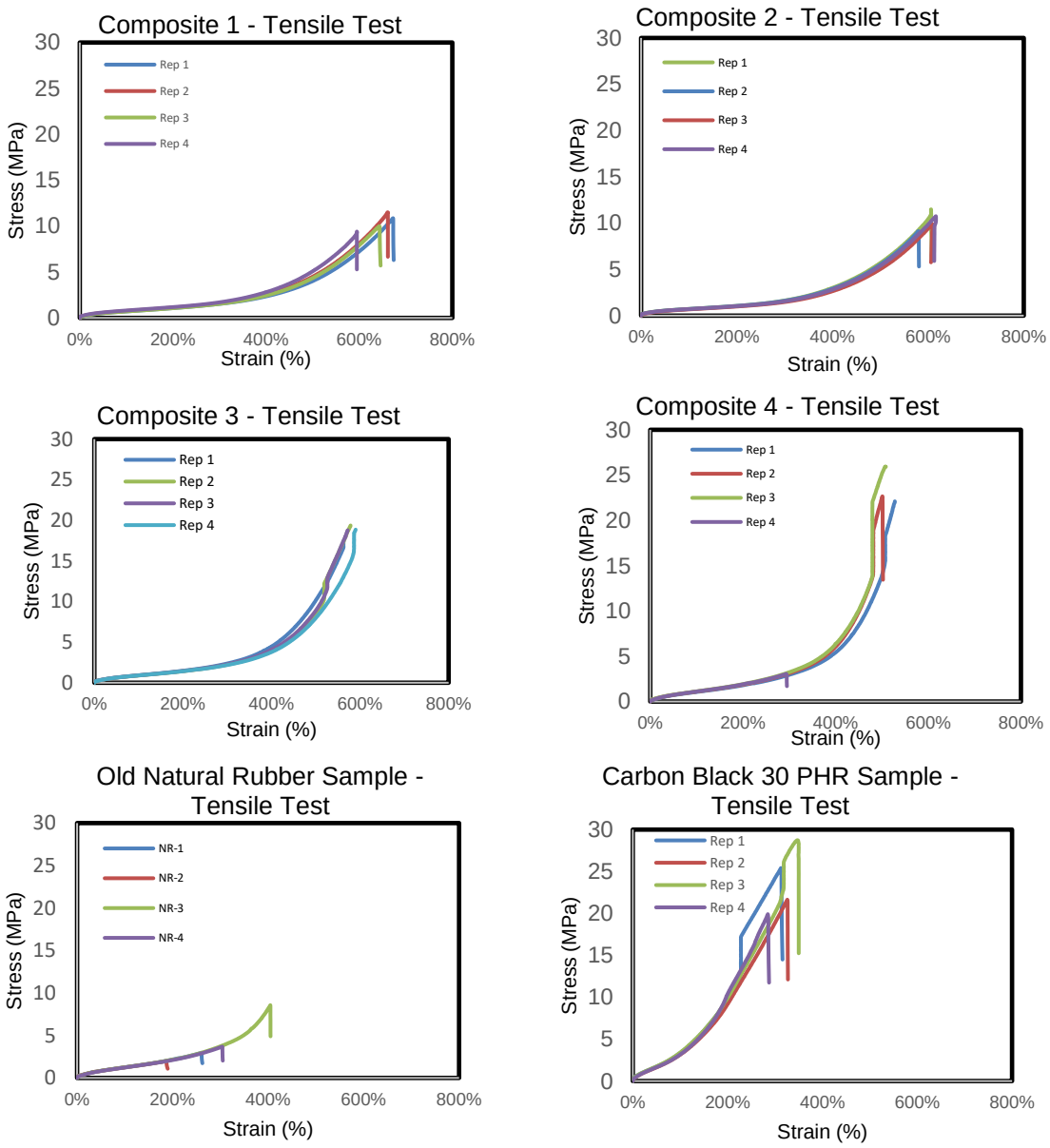

Figure 2-6. Stress-strain curves generated from tensile testing the glucose-rubber composites with natural rubber and carbon black controls.

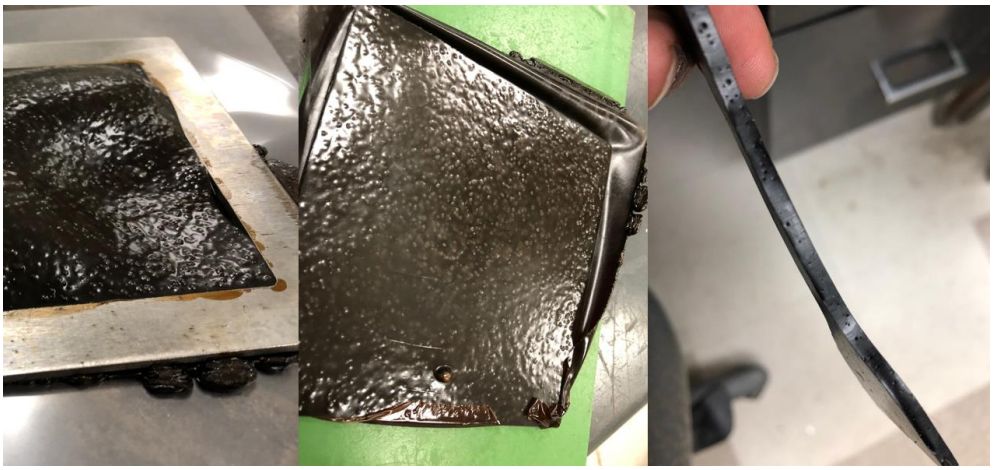

Figure 2-7. Composite 1, loaded with 12 grams of D-glucose (30 phr).

The sample shown in Figure 2-7 was shown to have a major presence of bubbles (presumed before this study to be trapped air), akin to the previous negative behavior seen in nanopectin and soy molasses samples compounded on our behalf by Dr. Jong at USDA earlier in 2018. Additionally, there were clear deformities and voids seen in the cross-section of these samples after die-cutting these samples into dumbell specimens.

Figure 2-8. The compression molded glucose-NR composite at 1.25 phr.

In contrast, the “bubbling” behavior seen in the 30 phr glucose-rubber composite was not seen in the composite that was loaded with 1.25 phr glucose (shown in Figure 8). This observation suggested that there was a critical level of glucose that allowed this phenomenon to happen and demonstrated the importance of removing excess sugars in our soybean hull and soybean flour systems. This showed that excess glucose in rubber could negatively affect the integrity of the rubber.

2.3.2.2 Sugar Leeching in Uncured Glucose-Rubber Composites

Table 2-4. Glucose leeching from uncured glucose-rubber composites in water.

Sample	Sugar in [g]	Percent Mass Lost %	Est. Sugar Content %
Composite 1	12.02	23.98	22.95
Composite 2	7.82	6.33	15.97
Composite 3	2.03	1.80	4.83
Composite 4	0.51	1.37	1.25

This table shows that when sugar exists above 7.82g in a natural rubber composite after mastication but before vulcanization, most of the sugar is leeched from the oven dried latex. This suggests that simply adjusting pH, mixing, and blending this aqueous solution with natural rubber latex did little to help rubber-filler binding on a molecular level, as sugar was leeched out into water especially at higher concentrations. It was observed, however, after curing the rubber samples that no leeching occurred after immersion in water. It is likely that the cross-linking of sulfur during vulcanization may have trapped the glucose in the rubber composite.

2.3.3 Rubber Compounding Results with Soybean Hull Hydrolysate

Figure 2-9. Rubber with Blended Hydrolysate (left), Sonicated Hydrolysate (middle), Carbon Black (right).

Samples were compression molded in the same stainless steel mold. It is possible, much like the glucose-rubber composites that the brown coloration comes from Maillard browning from sugars and proteins in the hydrolysates even after they were washed.

2.3.3.1 Moving Die Rheometer Results of Soybean Hull Reinforced Composites

Finding the optimum curing time of rubber composites was critical for finding the robustness of each composite with regards to scorch time and learning the maximum cure time and behavior after this plateau. In Table 2-5, the MDR results presented an elementary prediction of these rubber samples' response and resistance to deformation.

Table 2-5. Moving die rheometer results for soybean hull rubber composites, natural rubber, and carbon black samples.

Sample	Optimum Curing Time (t90)	Max Torque (Nm)
Natural Rubber (control)	11.96 ± 0.71	8.86 ± 0.11
Natural Rubber with Blended Hydrolysate (30 phr)	6.87 ± 0.22	14.30 ± 0.26
Natural Rubber with Sonicated Hydrolysate (30 phr)	8.79 ± 0.48	12.69 ± 0.40
Natural Rubber with Carbon Black (30 phr)	6.59 ± 0.07	16.34 ± 0.08

2.3.3.2 Tensile Test Results for Soybean Hull Reinforced Composites

After vulcanizing these composites at the optimum cure times, these samples were tensile tested with the Instron. The values for stress and strain at break and the 100% and 300% moduli are shown in the table 2-6.

Table 2-6. Values for strain and stress at fracture and moduli for soybean hull rubber composites, natural rubber, and carbon black samples.

Sample	Max Stress UTS [MPa]	Tensile Strain at Break [%]	Tensile Stress at Break [Mpa]	100% Modulus [Mpa]	300% Modulus [Mpa]
Natural Rubber	17.62 ± 1.34	487.77 ± 37.15	15.71 ± 2.23	1.11 ± 0.09	2.98 ± 0.35
Natural Rubber + Blended Hydrolysate	18.55 ± 0.49	527.13 ± 13.37	18.55 ± 0.49	2.20 ± 0.08	4.79 ± 0.16
Natural Rubber + Sonicated Hydrolysate	18.26 ± 0.46	527.37 ± 29.64	18.20 ± 0.39	1.69 ± 0.05	3.95 ± 0.08
Natural Rubber + Carbon Black	28.65 ± 1.96	424.04 ± 27.80	28.33 ± 1.63	2.79 ± 0.13	16.51 ± 1.40

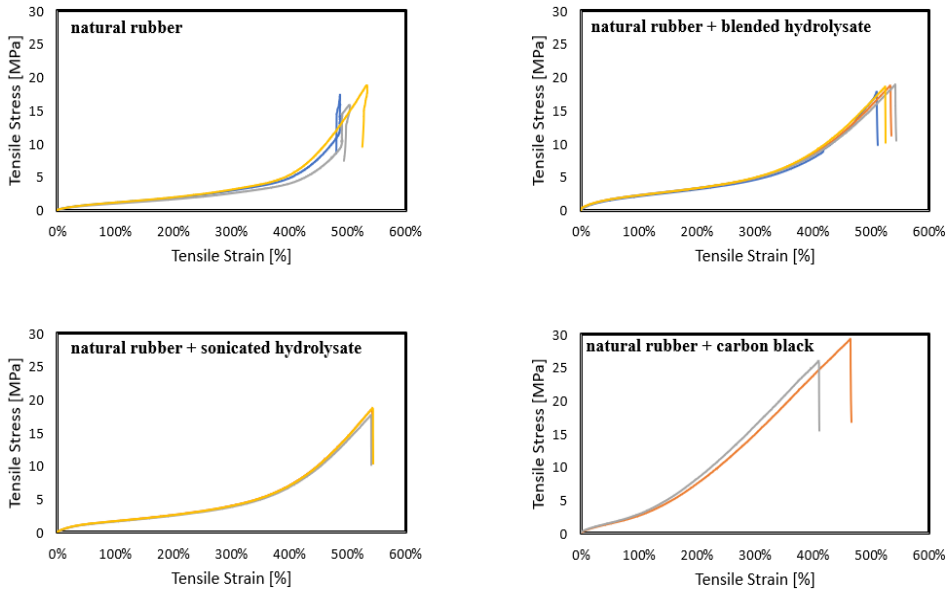

Figure 2-10. Stress-strain curves for the natural rubber control, the rubber with blended soy hull hydrolysate, the carbon black control sample, and the rubber with the sonicated soy hull hydrolysate.

The results in Table 2-6 for the ultimate tensile strength of the composites show that using 30 phr soy hull solids in natural rubber after enzyme hydrolysis, separation from soluble components, and blending and sonication treatments improves the tensile strength by 3 Mpa compared to natural rubber. In comparison, the natural rubber reinforced with carbon black fractures at a tensile stress approximately 1.5 times that of the natural rubber samples reinforced with soy hull particles. These results show that soy hull solids could not sufficiently reinforce natural rubber on the order of carbon black.

2.3.4 Reinvestigating Soy Flour Hydrolysate as a Rubber Filler

Preliminary experiments with the composites were tested with soy flour hydrolysate in the natural rubber to see how it affected performances. In these preliminary experiments, the rubber compounding process was still being learned and more focus was allocated towards effectively drying the composite. After the soybean hull solids showed minimal reinforcement of natural rubber, soy flour was once again investigated because of previous success of soy protein isolate in natural rubber (Jong, 2015). Dr. Jong's research showed that microfluidized soy protein isolate successfully reinforced natural rubber. In our process, the use of enzyme cocktail over acid hydrolysis continued to be the novelty of this project. For this reason, soy protein concentrate produced with the enzyme hydrolysis process detailed in Chapter I was investigated next as a possible reinforcing agent of natural rubber.

At this point in the project, a homogenizer was finally purchased and incorporated into this process for ease of particle size reduction. This disperser was much easier to use compared to the sonication device previously employed and also provided dispersion at speeds as high as 20000 rpm (as opposed to the shear provided by the Waring blender previously used). After homogenizing soy protein concentrate solids at alkali pH and mixing with natural rubber latex to dry overnight at two filler concentrations, 25 and 50 phr, more issues arose. The first issue with switching to soy flour once again was the presence of severe aggregation during drying. This drying issue was not previously seen when using soy flour hydrolysate in the initial experiments. The aggregation of this soy

protein concentrate resulted in strong adhesion to the glass pyrex tray. The brittle nature of this dried composite rendered the sample unfit for rubber compounding and proper mastication in the Brabender. To avoid this issue, three separate drying surfaces were investigated: the same glass dish coated with di-methyl siloxane (DMSO), another glass pyrex dish coated with soybean oil, and a polypropylene surface. It was found that release from the polypropylene surface was much friendlier to the dried SPC-rubber composite and the same brittle characteristics seen during drying in the glass surfaces was not observed. These rubber composites, at 25 phr and 50 phr of SPC loading, were successfully isolated after drying on this polypropylene surface, masticated in the Brabender, and cured in a compression mold. Unfortunately, this side-study with SPC as a filler was unable to be continued due to the COVID-19 lockdown that shutdown most of the labs and equipment necessary to analyze this system further.

2.4 Conclusions and Recommendations

As discussed in Chapter I, nanosized particles did exist in the soybean hull and soybean flour hydrolysate after washing soluble sugars and proteins and conducting mechanical treatment with the resuspended solids (sonication, blending, homogenization). However, the results presented in Chapter I concluded that the concentration of these nanosized particles was small relative to particles above 200 μm. Microscope pictures of the slurry showed the presence of macrosclereid structures that were cleaved from the seed coat and smaller fragments that were left unhydrolyzed. Even after further sonication and

homogenization, these particles were difficult to reduce to the nanoscale. The recovery from soybean hull after sonication and filtration through 2.7 µm showed a small yield of solids that would be insufficient for optimal mixing in the Brabender and vulcanization steps of this project. Eventually, due to the demands of the project funding at the time, these resuspended solids that contained more microparticles than nanosized solids were mixed and tested with natural rubber latex to study reinforcing properties.

The purpose of the initial tensile tests with soy flour hydrolysate was to become familiar with the rubber processing from start to finish, as well as see if reproducing Dr. Lei Jong's previous work with soy protein isolate could be reproduced using our enzyme hydrolysis and sonication process. Initial testing with soy flour hydrolysate (a well-studied system from previous members of our lab) showed minimal reinforcement of natural rubber. During these early experiments, the optimum cure time was also disregarded as a factor and the curing time was set at 15 minutes to maintain the same thermal history (Jong, 2015).

During these initial experiments, it was also realized that the rubber basis was supposed to be kept constant when changing the filler concentration in parts per hundred rubber. It was also understood after testing D-glucose as a filler in natural rubber that excess glucose posed a problem for the integrity and strength of the vulcanized rubber. The result of the glucose-composite study brought attention to the importance of separating soluble sugars (among other proteins and components) from the desired soybean solids. After these initial

experiments, soybean hull hydrolysate after washing away sugars was next further investigated once homogenization and blending were later studied to reduce particle size. Although nanoscale was not achieved, the importance of continuing rubber processing was important to satisfy the requirements of the project. When the soybean hull system was investigated, no positive reinforcement of the natural rubber was found at 30 phr loading. Elastic moduli showed that there was a plasticizing effect compared to the rigid carbon black samples when tensile tested. It was unclear based off the SEM imaging of the composite surfaces whether or not this plasticizing effect was due to the large size of particles in the solid suspensions, or lack of sufficient filler-filler and rubber-filler interactions that are necessary for reinforcing properties. Due to circumstances of COVID-19, tensile test results, SEM pictures, and further analysis of the protein and carbohydrates in the soybean hull solids after enzyme hydrolysis were unable to be studied further.

Future work should investigate both how to improve the yield and isolation of nanosized solids through staged filtration steps and iterations of homogenization. In order to improve filler-filler interactions, chemical modification of the rubber or the biomass-derived solid fillers with silanization or TEMPO oxidation is recommended. This would facilitate better interactions between the hydrophobic natural rubber and the hydrophilic filler suspensions. Furthermore, in future studies the rubber should be dried in the hood at ambient temperature to avoid side-reactions that occur at high temperature during oven drying, as well as prematurely aging the rubber before compounding. It is also suggested that in

the future, a smaller steel mold with 1-2 mm thickness is used. The samples generated in this study were thick (3.0 – 3.3 mm) in comparison, which rendered them difficult to test with dynamical mechanical analysis.

BIBLIOGRAPHY

Abraham, T. (2016). Thermoplastic Elastomers: Fundamentals, 139-208. In, Rogers, B. (Ed.), Rubber Compounding: Chemistry and Applications, Second Edition. CRC Press, Taylor & Francis Group LLC, Boca Raton, Florida.

Agbor, V.B., Cicek, N., Sparling, R., Berlin, & A., Levin, D.B. (2011). Biomass pretreatment: Fundamentals toward application. *Biotechnology Advances*, *29*, 675–685.

ASTM International. (2003). Standard test method for tensile properties of plastics. *ASTM International*, *08*, 46–58.

Brinchi, L., Cotana, F., Fortunati, E., Kenny, J.M. (2013). Production of nanocrystalline cellulose from lignocellulosic biomass: Technology and applications. *Carbohydrate Polymers*, *94*, 154–169.

Cai, J., & Zhang, L. (2006). Unique gelation behavior of cellulose in NaOH/urea aqueous solution. *Biomacromolecules*, *7*, 183–189.

Cai, J., Zhang, L., Zhou, J., Qi, H., Chen, H., Kondo, T., Chen, X., & Chu, B. (2007). Multifilament fibers based on dissolution of cellulose in NaOH/urea aqueous solution: structure and properties. *Advanced Materials*, *19*, 821–825.

Coffman, A. (2013). Production of Carbohydrases by Fungus *Trichoderma Reesei* Grown on Soy-based Media. Master's Thesis, University of Akron, Ohio. Retrieved from https://etd.ohiolink.edu/

Colvin, H. (2016). General Purpose Elastomers, 33-82. In, Rogers, B. (Ed.), Rubber Compounding: Chemistry and Applications, Second Edition. CRC Press, Taylor & Francis Group LLC, Boca Raton, Florida.

Curvello, R., Raghuwanshi, V. S., & Garnier, G. (2019). Engineering nanocellulose hydrogels for biomedical applications. *Advances in Colloid and Interface Science*, *267*, 47–61.

Dong, H., Strawhecker, K. E., Snyder, J. F., Orlicki, J. A., Reiner, R. S., & Rudie, A. W. (2012). Cellulose nanocrystals as a reinforcing material for electrospun poly(methyl methacrylate) fibers: Formation, properties and nanomechanical characterization. *Carbohydrate Polymers*, *87*, 2488–2495.

Ferreira, F. V, Mariano, M., Rabelo, S. C., Gouveia, R. F., & Lona, L. M. F. (2018). Applied Surface Science Isolation and surface modification of cellulose nanocrystals from sugarcane bagasse waste: From a micro- to a nano-scale view. *Applied Surface Science*, *436*, 1113–1122.

Flauzino Neto, W. P., Mariano, M., da Silva, I. S. V., Silvério, H. A., Putaux, J. L., Otaguro, H., Pasquini, D., & Dufresne, A. (2016). Mechanical properties of natural rubber nanocomposites reinforced with high aspect ratio cellulose nanocrystals isolated from soy hulls. *Carbohydrate Polymers*, *153*, 143–152.

Flauzino Neto, W.P., Silvério, H.A., Dantas, N.O., Pasquini, D. (2013). Extraction and characterization of cellulose nanocrystals from agro-industrial residue – soy hulls. *Industrial Crops and Products*, *42*, 480–488.

García, A., Gandini, A., Labidi, J., Belgacem, N., & Bras, J. (2016). Industrial and crop wastes: A new source for nanocellulose biorefinery. *Industrial Crops and Products*, *93*, 26–38.

George, J. & Sabapathi, S.N. (2015). Cellulose nanocrystals: synthesis, functional properties, and applications. *Nanotechnology, Science and Applications*, *8*, 45–54.

Ignatz-Hoover, F. & To, B.H. (2016). Vulcanization, 461-522. In, Rogers, B. (Ed.), Rubber Compounding: Chemistry and Applications, Second Edition. CRC Press, Taylor & Francis Group LLC, Boca Raton, Florida.

Isikgor, F. H., & Becer, C. R. (2015). Lignocellulosic biomass: a sustainable platform for the production of bio-based chemicals and polymers. *Polymer Chemistry*, *6*, 4497–4559.

Islam, S. M. M., Elliott, J. R., & Ju, L. K. (2018). Minimization of fermentation inhibitor generation by carbon dioxide-water based pretreatment and enzyme hydrolysis of guayule biomass. *Bioresource Technology*, *251*, 84-92.

Islam, S. M. M., Li, Q., Loman, A. Al, & Ju, L. K. (2017). CO2-H2O based pretreatment and enzyme hydrolysis of soybean hulls. *Enzyme and Microbial Technology*, *106*, 18–27.

Jiang, F., Hsieh, Y. (2013). Chemically and mechanically isolated nanocellulose and their self-assembled structures. *Carbohydrate Polymers*, *95*, 32–40.

Jong, L. (2013). Characterization of Soy Protein Nanoparticles Prepared by High Shear Microfluidization. *Journal of Dispersion Science and Technology*, *34*, 469–475.

Jong, L. (2015). Influence of protein hydrolysis on the mechanical properties of natural rubber composites reinforced with soy protein particles. *Industrial Crops and Products*, *65*, 102–109.

Jong, L. (2017). Reinforcement effect of soy protein nanoparticles in amine-modified natural rubber latex. *Industrial Crops and Products*, *105*, 53–62.

Jong, L. (2018). Improved natural rubber composites reinforced with a complex filler network of biobased nanoparticles and ionomer. *Materials Chemistry and Physics*, *203*, 156–165.

Kalia, S., Dufresne, A., Cherian, B.M., Kaith, B.S., Averous, L., Njuguna, J., & Nassiopoulos, E. (2011). Cellulose-Based Bio- and Nanocomposites: A Review. *International Journal of Polymer Science*, 1-39.

Kargarzadeh, H., Huang, J., Lin, N., Ahmad, I., Mariano, M., Dufresne, A., … Gałęski, A. (2018). Recent developments in nanocellulose-based biodegradable polymers, thermoplastic polymers, and porous nanocomposites. *Progress in Polymer Science*, *87*, 197–227.

Karim, Z., Afrin, S., Husain, Q., & Danish, R. (2017). Necessity of enzymatic hydrolysis for production and functionalization of nanocelluloses. *Critical Reviews in Biotechnology*, *37*, 355–370.

Li, Q., Loman, A. Al, Callow, N. V., Islam, S. M. M., & Ju, L. K. (2018). Leveraging pH profiles to direct enzyme production (cellulase, xylanase, polygalacturonase, pectinase, A-galactosidase, and invertase) by Aspergillus foetidus. *Biochemical Engineering Journal*, *137*, 247–254.

Li, Q., Loman, A. Al, Coffman, A. M., & Ju, L. K. (2017). Soybean hull induced production of carbohydrases and protease among Aspergillus and their effectiveness in soy flour carbohydrate and protein separation. *Journal of Biotechnology*, *248*, 35–42.

Li, Q., Ray, C. S., Callow, N. V, Loman, A. A., Islam, S. M. M., & Ju, L. K. (2020). Enzyme and Microbial Technology Aspergillus niger production of pectinase and α -galactosidase for enzymatic soy processing. *Enzyme and Microbial Technology*, *134*, 1–7.

Loman, A. A. & Ju, L. K. (2017). Enzyme-based processing of soybean carbohydrate: Recent developments and future prospects. *Enzyme and Microbial Technology*, *106*, 35–47.

Loman, A. A., & Ju, L. K. (2016). Soybean carbohydrate as fermentation feedstock for production of biofuels and value-added chemicals. *Process Biochemistry*, *51*, 1046–1057.

Loman, A. A., Islam, S. M. M., Li, Q., & Ju, L. K. (2016). Soybean bio-refinery platform: enzymatic process for production of soy protein concentrate, soy protein isolate and fermentable sugar syrup. *Bioprocess and Biosystems Engineering*, *39*, 1501–1514.

Loman, A. Al, Islam, S. M. M., Li, Q., & Ju, L.K. (2017). Enzyme recycle and fed-batch addition for high-productivity soybean flour processing to produce enriched soy protein and concentrated hydrolysate of fermentable sugars. *Bioresource Technology*, *241*, 252–261.

Lu, P. & Hsieh, Y.L. (2010). Preparation and properties of cellulose nanocrystals: Rods, spheres, and network. *Carbohydrate Polymers*, *82*, 329-336.

Lu, P., & Hsieh, Y. Lo. (2010). Preparation and properties of cellulose nanocrystals: Rods, spheres, and network. *Carbohydrate Polymers*, *82*, 329–336.

Ma, F., Cholewa, E., Mohamed, T., Peterson, C. A., & Gijzen, M. (2004). Cracks in the palisade cuticle of soybean seed coats correlate with their permeability to water. *Annals of Botany*, *94*, 213–228.

Martelli-Tosi, M., Torricillas, M. da S., Martins, M. A., Assis, O. B. G. de, & Tapia-Blácido, D. R. (2016). Using Commercial Enzymes to Produce Cellulose Nanofibers from Soybean Straw. *Journal of Nanomaterials*, 1–10.

Merci, A., Urbano A., Grossman M.V. E., Tischer C.A., & Mali, S. (2015). Properties of microcrystalline cellulose extracted from soybean hulls by reactive extrusion. *Food Research International*, *73*, 38-48.

Mishra, R. K., Sabu, A., & Tiwari, S. K. (2018). Materials chemistry and the futurist eco-friendly applications of nanocellulose: Status and prospect. *Journal of Saudi Chemical Society*, *22*, 949–978.

Mishra, R. K., Sabu, A., & Tiwari, S. K. (2018). Materials chemistry and the futurist eco-friendly applications of nanocellulose: Status and prospect. Journal of Saudi Chemical Society, 22, 949–978.

Missoum, K., Belgacem, M. N., & Bras, J. (2013). Nanofibrillated cellulose surface modification: A review. *Materials*, *6*, 1745–1766.

Moneypenny, H.G., Menting, K., & Gragg, F.M. (2016). General Compounding, 333-378. In, Rogers, B. (Ed.), Rubber Compounding: Chemistry and Applications, Second Edition. CRC Press, Taylor & Francis Group LLC, Boca Raton, Florida.

O'Bryan, C. A., Kushwaha, K., Babu, D., Crandall, P.G., Davis, M.L., Chen, P., Lee, S., Ricke, S.C. (2014). Soybean Seed Coats: A Source of Ingredients for Potential Human Health Benefits-A Review of the Literature. *Journal of Food Research*, *3*, 188–200.

Peng, Y., Gardner, D.J., & Han, Y. (2012). Drying cellulose nanofibrils: in search of a suitable method. *Cellulose*, *19*, 91–102.

Phanthong, P., Reubroycharoen, P., Hao, X., Xu, G., Abudula, A., Guan, G. (2018). Nanocellulose: Extraction and application. *Carbon Resources Conversion*, *1*, 32–43.

Rånby, B. G. (1951) Fibrous Macromolecular Systems. Cellulose and Muscle. The Colloidal Properties of Cellulose Micelles. *Discuss. Faraday Soc.* 1951, 11, 158-164.

Rogers, B. (2016). Natural Rubber and Other Naturally Occurring Compounding Materials, 1–32. In, Rogers, B. (Ed.), Rubber Compounding: Chemistry and Applications, Second Edition. CRC Press, Taylor & Francis Group LLC, Boca Raton, Florida.

Wampler, W.A., Nikiel, L., & Evans, E.N. (2016). Carbon Black, 209-250. In, Rogers, B. (Ed.), Rubber Compounding: Chemistry and Applications, Second Edition. CRC Press, Taylor & Francis Group LLC, Boca Raton, Florida.

Wang, Q., Wei, W., Chang, F., Sun, J., Xie, S., & Zhu, Q. (2016). Controlling the Size and Film Strength of Individualized Cellulose Nanofibrils Prepared by Combined Enzymatic Pretreatment and High Pressure Microfluidization. *BioResources*, *11*, 2536–2547.

Xie, Y., Hill, C. A. S., Xiao, Z., Militz, H., & Mai, C. (2010). Silane coupling agents used for natural fiber/polymer composites: A review. *Composites Part A: Applied Science and Manufacturing*, *41*, 806–819.